Article

SOURCE DATA | TRANSPARENT PROCESS

EMBO reports

p53 gain-of-function mutations increase Cdc7-dependent replication initiation

Arindam Datta[1,†], Dishari Ghatak[1,†], Sumit Das[2], Taraswi Banerjee[3], Anindita Paul[4], Ramesh Butti[2], Mahadeo Gorain[2], Sangeeta Ghuwalewala[1], Anirban Roychowdhury[5], Sk Kayum Alam[1], Pijush Das[1], Raghunath Chatterjee[6], Maitrayee Dasgupta[4], Chinmay Kumar Panda[5], Gopal C Kundu[2] & Susanta Roychoudhury[1,7,*]

Abstract

Cancer-associated p53 missense mutants confer *gain of function* (GOF) and promote tumorigenesis by regulating crucial signaling pathways. However, the role of GOF mutant p53 in regulating DNA replication, a commonly altered pathway in cancer, is less explored. Here, we show that enhanced Cdc7-dependent replication initiation enables mutant p53 to confer oncogenic phenotypes. We demonstrate that mutant p53 cooperates with the oncogenic transcription factor Myb *in vivo* and transactivates Cdc7 in cancer cells. Moreover, mutant p53 cells exhibit enhanced levels of Dbf4, promoting the activity of Cdc7/Dbf4 complex. Chromatin enrichment of replication initiation factors and subsequent increase in origin firing confirm increased Cdc7-dependent replication initiation in mutant p53 cells. Further, knockdown of *CDC7* significantly abrogates mutant p53-driven cancer phenotypes *in vitro* and *in vivo*. Importantly, high *CDC7* expression significantly correlates with p53 mutational status and predicts poor clinical outcome in lung adenocarcinoma patients. Collectively, this study highlights a novel functional interaction between mutant p53 and the DNA replication pathway in cancer cells. We propose that increased Cdc7-dependent replication initiation is a hallmark of p53 *gain-of-function* mutations.

Keywords Cdc7-Dbf4; gain-of-function; mutant p53; origin firing; replication
Subject Categories Cancer; DNA Replication, Repair & Recombination; Signal Transduction
DOI 10.15252/embr.201643347 | Received 13 September 2016 | Revised 4 August 2017 | Accepted 9 August 2017 | Published online 8 September 2017
EMBO Reports (2017) 18: 2030–2050

Introduction

The majority of the human cancers harbors *TP53* mutation [1]. These are mostly missense mutations that result in full-length p53 proteins with altered function. The six "hot spot" residues (R175, G245, R248, R249, R273, and R282) of p53 DNA binding domain are frequently mutated in cancer [2]. Besides losing tumor suppressor function, these hot spot mutants gain novel oncogenic properties, defined as mutant p53 gain of function (GOF), and have been broadly categorized as contact (R248W, R248Q, and R273H) or structural (G245S, R249S, R282H, and R175H) mutants depending on the function of the residues altered [2]. Importantly, data from cell-based assays as well as from animal model experiments suggest that mutants from these two classes differ in terms of GOF phenotypes [2,3]. For example, p63/p73 interacts with both structural and contact mutants, albeit less effectively with the latter [2,4]. Selective gain-of-function effect also has been reported in the context of chemoresistance. Whereas mutant $p53^{R175H}$ has been shown to confer substantial resistance to etoposide in cultured cancer cells, mutant $p53^{R273H}$ showed less protective effect [5]. It has been suggested that the molecular mechanism underlying GOF varies with different p53 mutants, which can be attributed to the differences in structural alterations caused by different mutations [3]. Cancer-associated GOF p53 mutants promote several cancer phenotypes including increased cellular growth, invasion and metastasis, genomic instability, deregulated energy metabolism, and enhanced chemoresistance [2]. By acting as an "oncogenic transcription factor", GOF mutant p53 transactivates a number of signaling genes by cooperating with other cellular transcription factors such as Ets-2, Sp1, NF-Y, VDR, SREBP, and Nrf2 [2,6]. Although several signaling pathways involved in mutant p53 gain of functions have been identified, many are still unexplored [2].

1 Cancer Biology and Inflammatory Disorder Division, CSIR-Indian Institute of Chemical Biology, Kolkata, India
2 Laboratory of Tumor Biology, Angiogenesis and Nanomedicine Research, National Centre for Cell Science (NCCS), Pune, India
3 Laboratory of Molecular Gerontology, National Institute on Aging, NIH Biomedical Research Center, NIH, Baltimore, MD, USA
4 Department of Biochemistry, University of Calcutta, Kolkata, India
5 Department of Oncogene Regulation, Chittaranjan National Cancer Institute, Kolkata, India
6 Human Genetics Unit, Indian Statistical Institute, Kolkata, India
7 Saroj Gupta Cancer Centre and Research Institute, Kolkata, India
*Corresponding author. Tel: +91 33 24995823; Fax: +91 33 24735197; E-mail: susantarc@gmail.com
†These authors contributed equally to this work

Recent study by Polotskaia *et al* [7] suggests that DNA replication pathway might be a crucial target of mutant p53. DNA replication is a tightly coordinated process that allows accurate duplication of the entire genome only once per cell division cycle. Errors in DNA replication lead to genomic instability and neoplastic transformation [8]. Genes involved in replication are often overexpressed in cancer tissues and chromatin enrichment of pre-replicative complex (pre-RC) proteins has been reported in transformed cells compared to their normal counterparts [9]. Moreover, cancer cells utilize a significantly higher number of replication origins than normal cells [10]. Replication starts from thousands of replication origins distributed over the genome by the sequential and coordinated action of several replication factors [8]. One such factor is Cdc7, which is frequently overexpressed in various cancer cell lines and primary tumor tissues [11].

Originally isolated in budding yeast, Cdc7 is a conserved serine/threonine kinase required for replication initiation in vertebrates [12]. At the G1/S transition, Cdc7 binds to its regulatory subunit protein Dbf4 to form active DDK (Dbf4-dependent kinase) complex and triggers early as well as late origin firing throughout the S-phase [13]. In early G1-phase, origin recognition complex (ORC) along with Cdt1 and Cdc6 facilitates the loading of Mcm2-7 helicase on chromatin, which constitutes "licensed" pre-RCs. The individual origins are activated and "fired" in S-phase upon phosphorylation of Mcm proteins by Cdc7 and other S-phase CDKs followed by the subsequent recruitment of initiation factors Cdc45 and GINS [13]. Besides its conserved role in replication initiation, Cdc7 is also involved in DNA damage response (DDR) and helps maintain genome integrity under replication stress [14]. Deregulated Cdc7 activity has been implicated in advanced clinical stage, aneuploidy, survival, and chemoresistance in various cancer types, including oral cancer, ovarian cancer, colorectal cancer, melanoma, and breast cancer [15]. Notably, high Cdc7 expression often correlates with p53 mutation [11].

In this study, we elucidated the regulation of Cdc7 kinase by GOF mutant p53 and demonstrated Cdc7-dependent increased replication initiation in cancer cells harboring mutant p53. DNA replication was enriched as the most over-represented pathway with significant upregulation of Cdc7 kinase in GOF mutant p53-harboring lung cancer patients. We showed that GOF mutant p53 transactivates *CDC7* by cooperating with oncogenic transcription factor Myb in cancer cells. In addition, mutant p53 cells showed increased level of Dbf4 protein, the regulatory subunit of Cdc7 kinase. Importantly, mutant p53-expressing non-small cell lung carcinoma (NSCLC) cells showed increased replication initiation in a Cdc7-dependent manner. We further investigated the contribution of Cdc7 kinase to mutant p53 gain of functions both *in vitro* and *in vivo* and explored its significance in predicting clinical outcome of NSCLC patients. Collectively, our results demonstrate Cdc7-dependent altered replication initiation as a novel gain-of-function property of mutant p53.

Results

Increased *CDC7* expression in GOF mutant p53 cells

Given the well-defined role of GOF mutant p53 as an oncogenic transcription factor (TF) and the high prevalence of p53 mutation in lung cancer, we explored the possible mutant p53 targetome in TCGA lung adenocarcinoma (LUAD) cohort. Functional annotation of the differentially regulated genes (fold change ≥ 1.5, P-value < 0.01) between patients with wild-type and GOF mutant p53 ranked DNA replication as the most significantly enriched pathway in LUAD patients harboring GOF mutant p53 (Fig EV1A, Datasets EV1 and EV2). We found that genes enriched in this pathway are particularly involved in the initiation step of DNA replication (Dataset EV2). Among these genes, initiation factor Cdc7 kinase, which showed significantly higher expression in patients with GOF mutant p53 (Fig 1A), had been reported to be frequently overexpressed in multiple cancer cell lines and tumor specimens with p53 mutation [11]. We anticipated that GOF mutant p53 might positively regulate Cdc7 expression in cancer cells and therefore examined the effect of tumor-derived common p53 mutants on Cdc7 expression in p53-null NSCLC cell line, H1299. Compared to the control vector-infected cells (EV), increased Cdc7 expression at both RNA and protein levels was observed in mutant p53-R175H- and p53-R273H-expressing H1299 stable cells (Fig 1B and C). Similar results were

Figure 1. Increased Cdc7 expression in cancer cells harboring GOF mutant p53.

A Box–whisker plot showing relative *CDC7* expression (normalized read counts) in TCGA lung adenocarcinoma patients with wild-type and GOF mutant p53. The lower, middle and upper horizontal lines of the boxes indicate 25th, 50th (median) and 75th percentiles of the dataset respectively. The upper whisker represents maximum observed value below 1.5 IQR (interquartile range) and the lower whisker represents minimum observed value above 1.5 IQR. Mann–Whitney test was used to compute statistical significance. *P*-value is indicated.

B Relative mRNA expression of *CDC7* in H1299 cells either harboring empty vector (EV) or stably expressing GOF mutant p53-R175H and p53-R273H (upper panel). Levels of mutant p53 protein in stable cell lines were verified by immunoblotting (lower panel).

C Immunoblots showing Cdc7 protein level in control and mutant p53-expressing H1299 stable cells.

D Relative mRNA expression of *CDC7* and *DBF4* upon ectopic expression of wild-type p53, mutant p53-R175H, and p53-R273H in H1299 cells (upper and middle panels, respectively). Ectopic expression of wild-type and mutant p53 was verified by immunoblotting (lower panel).

E Immunoblots showing Cdc7 protein levels upon ectopic expression of mutant p53-R175H (left panel) and p53-R273H (right panel) in H1299 cells.

F Relative mRNA expression of *DBF4* in control (EV) and mutant p53-expressing H1299 stable cells.

G Immunoblots showing Dbf4 protein level in control and mutant p53-expressing H1299 stable cells.

H Immunoblots showing Dbf4 protein levels upon ectopic expression of mutant p53-R175H and p53-R273H in H1299 cells.

I Relative mRNA expression of *CDC7* in SkBr3 (left panel) and SW480 (right panel) cells upon shRNA-mediated knockdown of endogenous mutant p53.

J Immunoblots showing Cdc7 and Dbf4 protein levels upon stable knockdown of mutant p53 in SkBr3 (left panel) and SW480 (right panel) cells.

Data information: β-actin served as the loading control in immunoblots. Bar graphs represent mean ± SD; $n \geq 3$. (B, D, F, I) Two-tailed Student's *t*-test: *$P < 0.05$; ***$P < 0.001$; n.s., non-significant.
Source data are available online for this figure.

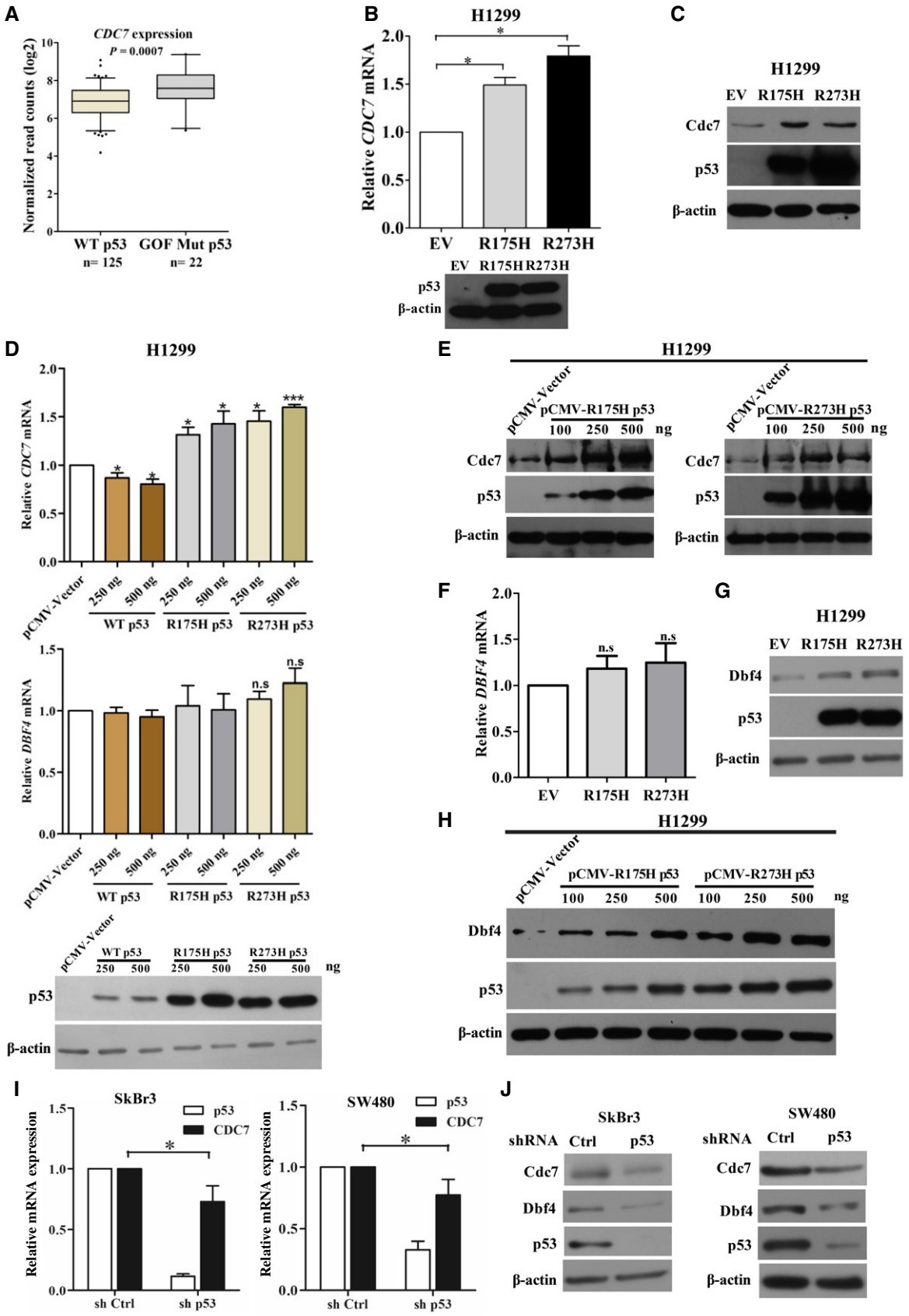

Figure 1.

obtained upon ectopic expression of these p53 mutants in H1299 as well as in colorectal cancer cell line HCT116 $p53^{-/-}$ (Figs 1D and E, and EV1B and C). In contrast, a small but significant decrease in *CDC7* mRNA level was observed upon ectopic expression of wild-type p53 in H1299 cells (Fig 1D), suggesting that the observed upregulation of *CDC7* in these cells is mutant p53 specific. Since along with Cdc7, its regulatory subunit Dbf4 is generally overexpressed in multiple human cancers, we next checked the RNA level of *DBF4* in presence of GOF mutant p53 [11]. However, *DBF4* was not enriched among the replication genes differentially regulated between TCGA patients with mutant and wild-type p53 (Dataset EV2). Also, we did not observe any significant change in *DBF4* transcript level either in mutant p53-expressing H1299 stable cells (Fig 1F) or upon ectopic expression of mutant or wild-type p53 in H1299 cells (Fig 1D). Interestingly, although mRNA levels were unchanged, we detected increased level of Dbf4 protein upon stable or transient expression of mutant p53 in these cells (Fig 1G and H). To ensure that the results obtained were not due to non-physiological level of p53, we compared the levels of ectopically expressed wild-type and mutant p53 in HCT116 $p53^{-/-}$ cells with that seen in tumor cell lines harboring endogenous p53. The levels of exogenously expressed wild-type and mutant p53 proteins were not found to be higher than those observed in cells expressing endogenous p53 (Fig EV1D). We also observed reduced expression of Cdc7 at both mRNA and protein levels upon stable knockdown of endogenous mutant p53 in breast cancer cell line SkBr3 (GOF mutant $p53^{R175H}$) and colorectal cancer cell line SW480 (GOF mutant $p53^{R273H}$; Fig 1I and J). siRNA-mediated transient knockdown of mutant p53 also led to reduced Cdc7 protein levels in these cell lines (Fig EV1E). Although mRNA levels were unchanged, substantial decrease in Dbf4 protein level was observed upon stable or transient knockdown of mutant p53 in these cell lines (Fig EV1F, J and G). Since Dbf4 level and Cdc7 activity peak at S-phase and maintained till the end of mitosis, it was important to see whether the results obtained were simply due to the higher fraction of S and G2/M population of mutant p53-expressing cells. Cell cycle profiles revealed that the percentage of S and G2/M population of mutant p53-expressing H1299 cells was not higher than that of control cells (Fig EV1H). Similarly, SkBr3 as well as SW480 cells showed similar cell cycle profile upon mutant p53 knockdown (Fig EV1I and J, respectively). These results suggest that the observed increase in Dbf4 and Cdc7 levels in mutant p53-expressing cells is not merely a reflection of changes in the cell cycle pattern, rather is mutant p53 dependent. Taken together, our observations suggest that mutant p53 upregulates *CDC7* expression and there is a simultaneous increase in the level of Dbf4 protein.

GOF mutant p53 interacts with Myb to transactivate *CDC7*

To investigate the underlying mechanism of regulation of Cdc7 kinase by GOF mutant p53, we measured *CDC7* promoter activity in cells expressing mutant p53. Compared to control cells, increased *CDC7* promoter activity was observed in mutant p53-R175H- and p53-R273H-expressing H1299 stable cell lines (Fig 2A). However, no significant change in *DBF4* promoter activity was observed in presence of mutant p53 (Fig 2B). Ectopic expression of p53 mutants also elicited a dose-dependent increase in *CDC7* promoter activity in H1299 cells (Fig 2C). In contrast, we observed a dose-dependent decrease in the promoter activity upon ectopic expression of wild-type p53, thereby suggesting a repressive effect of wild-type p53 on *CDC7* promoter (Fig 2C). Furthermore, stable knockdown of endogenous mutant p53 in SkBr3 and SW480 cells resulted in a significant decrease in *CDC7* promoter activity (Fig 2D). These results suggest that GOF p53 mutants can transactivate *CDC7* promoter in cancer cells. Mutant p53 proteins are known to interact with other cellular transcription factors and thereby enhance the expression of their respective target genes [2]. We therefore investigated for the possible transcription factor necessary for transactivation of *CDC7* by mutant p53. Oncogenic transcription factor Myb has been reported to be a direct transcriptional activator of *CDC7* [15,16]. Indeed, when we analyzed *CDC7* promoter region, we found two consensus binding sites of Myb (Figs 2E and EV2A). This prompted us to further investigate whether mutant p53 cooperates with Myb to drive *CDC7* expression in cancer cells. Results from ChIP-qPCR assay in H1299/R175H and H1299/R273H cells with or without mutant p53 knockdown showed selective enrichment of *CDC7* promoter sequences spanning Myb binding sites (−596 to −367 bp) in p53 immunoprecipitates (Fig 2F). On the contrary, no significant recruitment of mutant p53 was observed on distal *CDC7* promoter (−2,620 to −2,414 bp), 3′UTR of *CDC7* and *LMNB1* (Lamin B1) promoter, thereby suggesting the specificity of the recruitment. However, we could not detect any significant recruitment of wild-type p53 on *CDC7* promoter (Fig EV2B). Specific recruitment of endogenous mutant p53 on *CDC7* promoter was also

Figure 2. GOF mutant p53 transactivates *CDC7* and is recruited to its promoter via Myb.

A, B Relative *CDC7* (A) and *DBF4* (B) promoter activity in control and mutant p53-expressing H1299 stable cells.

C Relative *CDC7* promoter activity in control vector-, wild-type p53-, GOF mutant p53-R175H-, and p53-R273H-transfected H1299 cells (upper panel). Ectopic expression of p53 was verified by immunoblotting (lower panel).

D *CDC7* promoter activity upon stable knockdown of endogenous mutant p53 in SkBr3 and SW480 cells.

E Schematic representation of *CDC7* promoter harboring Myb binding sites. The Myb binding sites (−387 and −588 bp) wrt transcription start site (+1) are shown. Arrows represent pair of primers used to amplify *CDC7* promoter region spanning Myb consensus sequences in ChIP-qPCR assays.

F ChIP-qPCR showing mutant p53 recruitment on *CDC7* promoter (−596 to −367 bp) in H1299-R175H (upper panel) and H1299-R273H (lower panel) stable cells transfected with either control siRNA or *TP53* siRNA. Cells were transfected with 80 nM of siRNAs and incubated for 72 h before harvesting. Recruitment of mutant p53 on distal *CDC7* promoter (−2,620 to −2,414 bp), *CDC7* 3′ UTR, and *LMNB1* promoter is shown.

G ChIP-qPCR showing relative changes in mutant p53 recruitment on *CDC7* promoter (−596 to −367 bp) upon *MYB* knockdown in H1299-R175H (upper panel) and H1299-R273H (lower panel) stable cells. Cells were transfected with 80 nM of either control siRNA or *MYB* siRNA and harvested 72 h post-transfection.

Data information: β-actin served as the loading control. Bar graphs represent mean ± SD; $n = 3$; two-tailed Student's *t*-test: $^*P < 0.05$, $^{**}P < 0.01$, $^{***}P < 0.001$, n.s., non-significant.
Source data are available online for this figure.

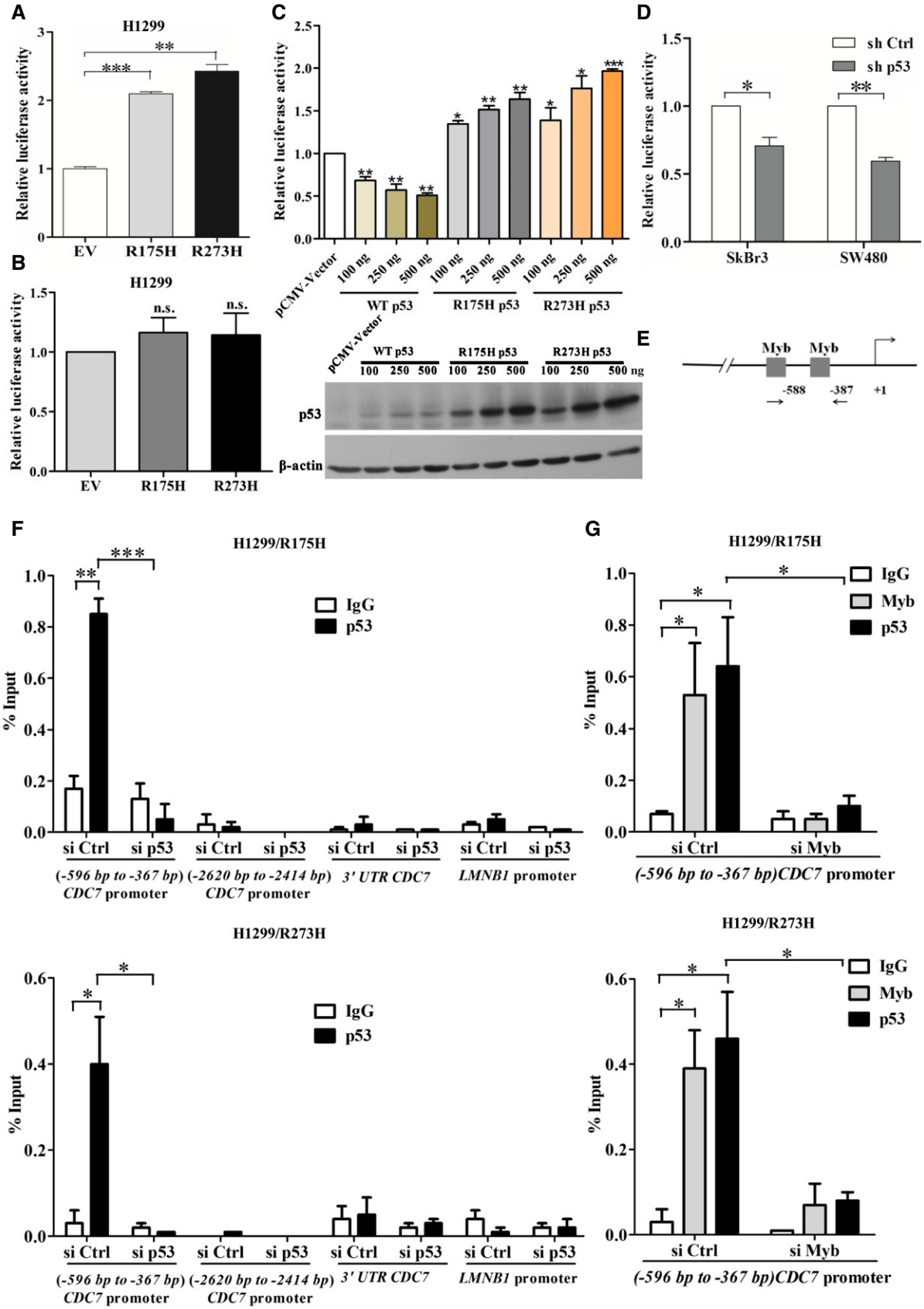

Figure 2.

observed in SkBr3 and SW480 cells (Fig EV2C and D, respectively). Importantly, knockdown of Myb significantly abrogated mutant p53 recruitment on *CDC7* promoter in H1299 cells, thereby suggesting the recruitment is Myb dependent (Appendix Fig S1A and Fig 2G). In support of this hypothesis, co-immunoprecipitation assays in mutant p53-expressing H1299 cells as well as in SkBr3 and SW480 cells confirmed that mutant p53 physically interacts with Myb *in vivo* (Fig 3A and B). We also detected wild-type p53 in Myb immunoprecipitates from HCT116 cells treated with 5-fluorouracil (5-FU; Fig 3C), which is consistent with the previous reports describing *in vivo* interaction between wild-type p53 and Myb [17,18]. We further attempted to identify the domain of mutant p53 required for the interaction with Myb. Results from co-immunoprecipitation experiments in H1299 cells co-transfected with Myb and either full-length mutant p53-R175H or its different mutant derivatives (Fig EV2E) showed reduced interaction upon deletion of a region between amino acid residues 355 and 338 of the tetramerization domain of mutant p53 (Fig 3D). The observation suggests that the tetramerization domain, which has been previously shown to mediate interaction with other factors including YAP and ETS2, might be important to form complex with Myb [19,20]. Next, we investigated the possible role of Myb in mediating mutant p53-driven transactivation of *CDC7*. Knockdown of Myb led to a significant decrease in enhanced *CDC7* promoter activity in mutant p53-expressing H1299 cells (Fig 3E). Further, unlike wild-type promoter (p*CDC7*-LucWT), activity of the *CDC7* promoter deleted of region flanking Myb binding sites (p*CDC7*-LucΔMyb) was not significantly increased in H1299 cells stably expressing p53-R175H (Appendix Fig S1B and C). Similar observation was obtained upon ectopic expression of this p53 mutant in these cells (Appendix Fig S1D). Deletion of Myb binding sequences also led to a significant reduction in basal *CDC7* promoter activity in control H1299 cells (Appendix Fig S1C and D). To further strengthen our observations, we introduced point mutations in the individual Myb binding sites on *CDC7* promoter (Constructs S1, S2, and S2+S1 in Fig 3F) and performed luciferase assay in control and mutant p53-expressing H1299 cells. Mutations in either distal (S1) or proximal (S2) Myb binding sites led to a significant reduction in basal *CDC7* promoter activity in control H1299 cells (Fig 3G), further suggesting Myb as a positive regulator of *CDC7* expression. Compared to the wild-type *CDC7* promoter (WT), mutant promoter with either distal (S1) or proximal (S2) site mutation showed attenuated transactivation by mutant p53 (Fig 3G). Although not completely abolished, the increase in *CDC7* promoter activity by mutant p53 was further reduced upon mutation in both distal and proximal Myb binding sites (S2+S1; Fig 3G). Similar observation was obtained upon ectopic expression of mutant p53-R175H in H1299 cells transfected with either wild-type (WT) or Myb site-mutated (S1, S2, and S2+S1) promoter constructs (Fig EV2F). Accordingly, the increase in *CDC7* mRNA level was found to be significantly compromised upon Myb knockdown in mutant p53-expressing H1299 cells (Fig EV2G). As expected, the basal-level expression of *CDC7* was also reduced in control H1299/EV cells upon Myb knockdown (Appendix Fig S1E). These data suggest an important contribution of Myb to mutant p53-driven transactivation of *CDC7* promoter and also indicate that there could be some other modes of regulation exist.

Increased level of Cdc7-Dbf4 complex and chromatin enrichment of phosphorylated Mcm2 and Cdc45 in GOF mutant p53 cells

We next investigated whether increased level of Cdc7 and Dbf4 correlates with higher amount of Cdc7/Dbf4 kinase complexes (DDK) in mutant p53-expressing cells. To this end, DDK complexes were immunoprecipitated from control and mutant p53-expressing H1299 stable cells using anti-Dbf4 antibody (Fig 4A). Correlating with increased levels of Cdc7 and Dbf4, increased amount of DDK complex was recovered from mutant p53-expressing cells than that from control cells (Fig 4A). We also checked whether mutant p53 is a part of Cdc7/Dbf4 complex. However, we could not detect p53 in Dbf4 immunoprecipitates (Fig 4A). Higher amount of DDK complex was also recovered from H1299 cells ectopically expressing mutant p53-R175H and p53-R273H (Fig 4B and C, respectively). Furthermore, we detected reduced amount of the kinase complex in SW480

Figure 3. GOF mutant p53 cooperates with Myb to transactivate *CDC7*.

A Co-immunoprecipitation assays showing interaction between mutant p53 and Myb in H1299-R175H (upper panel) and H1299-R273H (lower panel) stable cells. Mutant p53-Myb complexes were immunoprecipitated using anti-Myb antibody and subsequently detected with anti-p53 antibody in Western blotting.

B Co-immunoprecipitation assays showing interaction between endogenous mutant p53 and Myb in SkBr3 (upper panel) and SW480 (lower panel) cells. The experiment was performed as described in (A).

C Co-immunoprecipitation assays showing wild-type p53 and Myb interaction. HCT116 cells were treated with 5-FU for 24 h, and immunoprecipitation was done with anti-Myb antibody followed by Western blotting with anti-Myb and anti-p53 antibodies.

D H1299 cells were transfected with plasmid encoding Myb along with HA-tagged p53-R175H, p53-R175H Δproline, p53-R175H (1–338), p53-R175H (1–355), and p53-R175H (22,23) plasmid constructs. Cells were harvested 48 h post–transfection, and 1,000 μg of total protein from each sample was subjected to immunoprecipitation using anti-cMyb antibody or control rabbit serum IgG. Immunoprecipitated protein samples were run on 10% SDS–PAGE and transferred to PVDF membrane before blotting with anti-p53 and anti-Myb antibodies. Membrane with vector control, p53-R175H, p53-R175H Δproline, p53-R175H (1–338), and p53-R175H (1–355) samples was immunoblotted with anti-p53 (DO-1). Since p53-R175H (22,23) is not recognized by p53 (DO-1), the membrane containing the sample was blotted with anti-p53(Pab-240) antibody. Due to problem of IgG heavy chain with anti-p53 (Pab-240) antibody, the membrane was cut through the molecular weight marker and blotted separately. Levels of mutant p53 and Myb in input fractions are shown. IgG heavy chain and molecular weight marker are indicated. *Points to the specific bands.

E *CDC7* promoter activity upon *MYB* knockdown in control and mutant p53-expressing H1299 stable cells.

F Schematic showing wild-type (WT) and Myb site-mutated (S1, S2, and S2+S1) promoter luciferase constructs. The mutated nucleotides are shown in red.

G Relative luciferase activity of wild-type and Myb site-mutated *CDC7* promoter constructs in H1299-EV and H1299-R175H stable cells. Cells were transfected with 100 ng of each luciferase construct along with 25 ng of control pRL-TK plasmid. Twenty-four hour post-transfection, cells were harvested and dual-luciferase assay was performed.

Data information: Bar graphs represent mean ± SD; $n \geq 3$; two-tailed Student's *t*-test: *$P < 0.05$, **$P < 0.01$.
Source data are available online for this figure.

cells upon stable or transient knockdown of mutant p53 (Figs 4D and EV2H, respectively).

Since, along with increased amount of Cdc7 and Dbf4 proteins, mutant p53 cells showed relatively higher abundance of DDK complex, we next looked into the possible effect of GOF mutant p53 on replication initiation events downstream of Cdc7 kinase. Activated Cdc7 kinase specifically phosphorylates subunits of replicative helicase protein complex Mcm2-7, thereby facilitating local unwinding of DNA at individual replication origins, a prerequisite for replication initiation [13,21]. Among the Mcm subunits, Mcm2 is one of

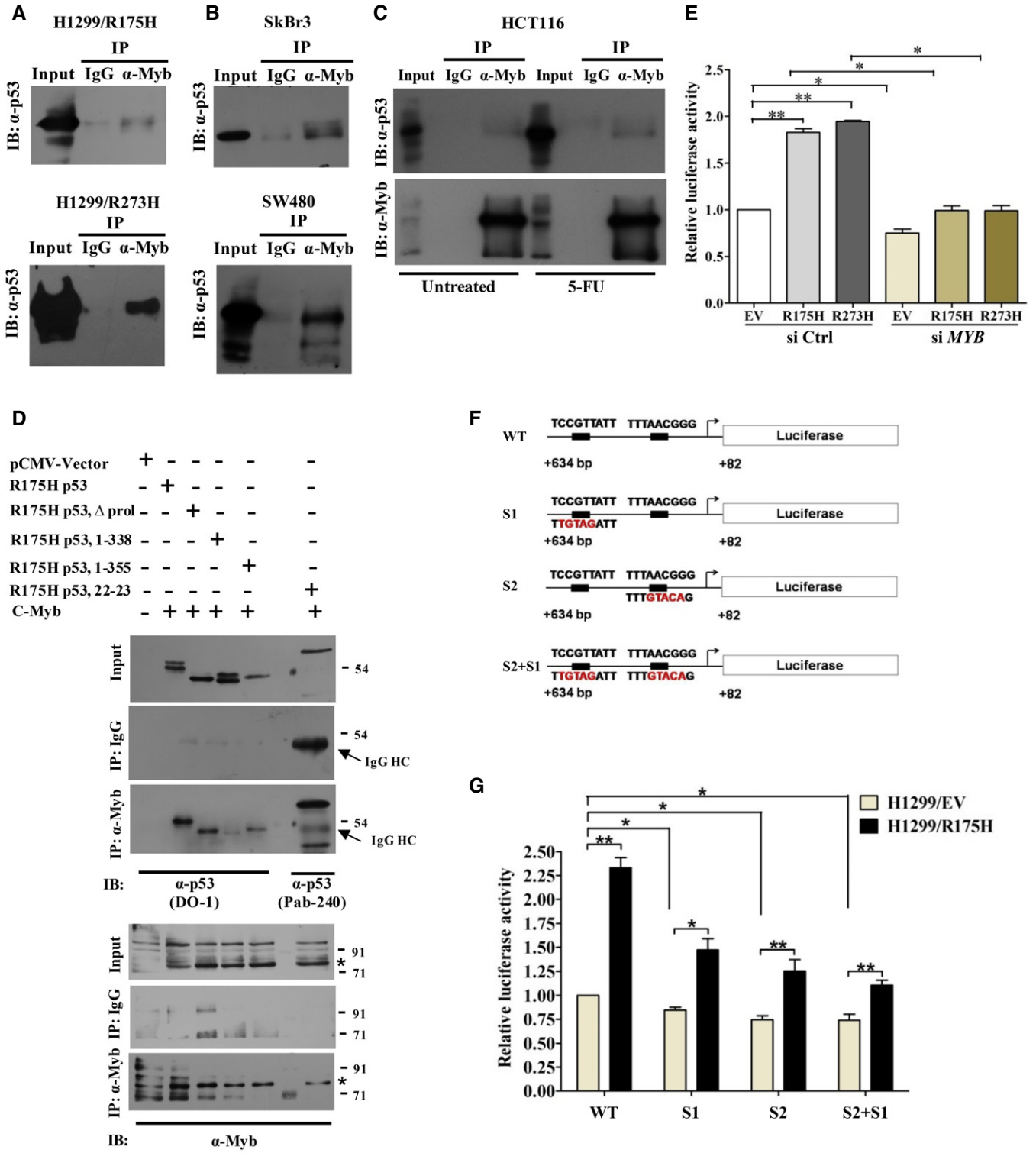

Figure 3.

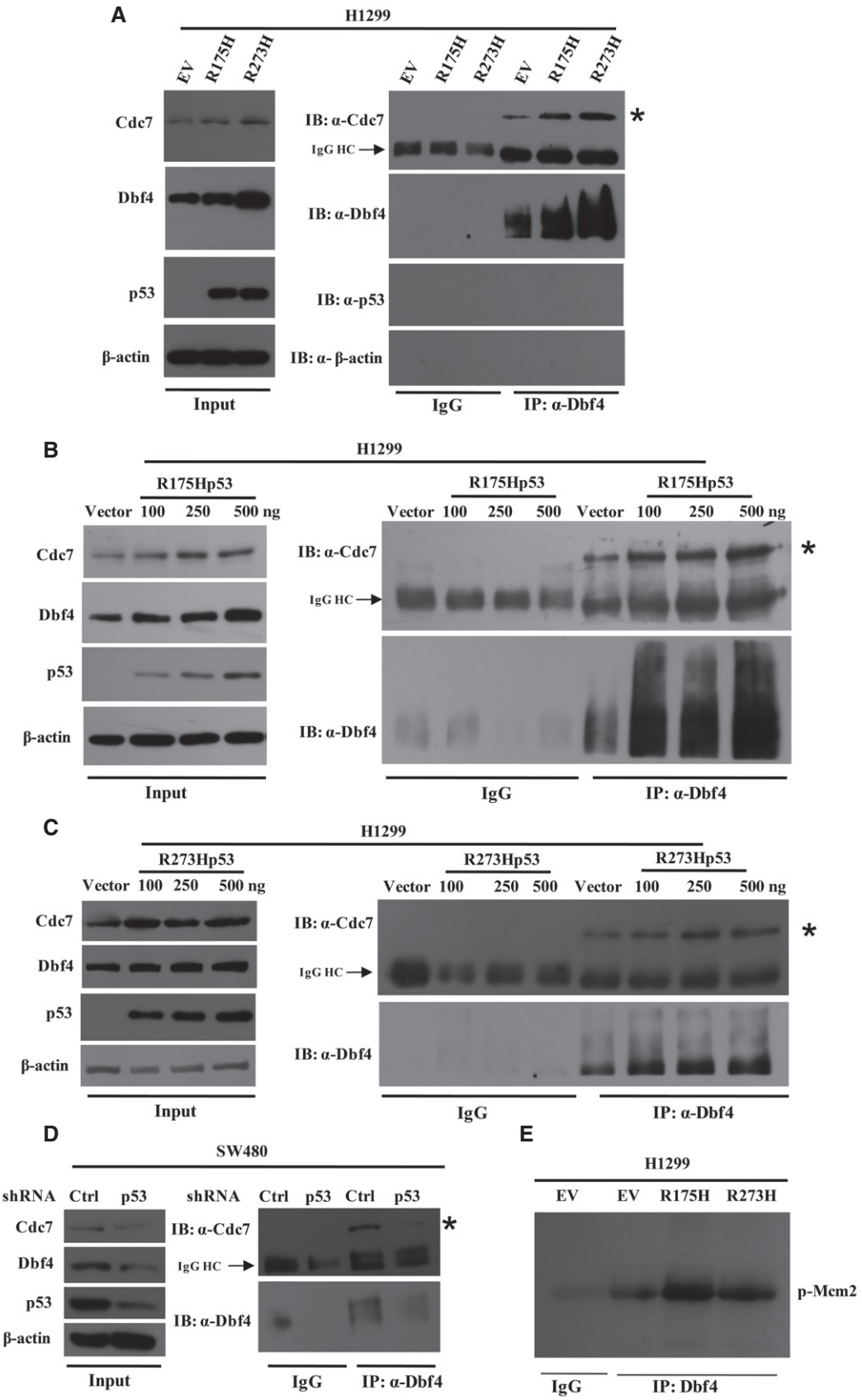
A
H1299
EV
R175H
R273H
Cdc7
Dbf4
p53
β-actin
Input
IB: α-Cdc7
IgG HC
IB: α-Dbf4
IB: α-p53
IB: α- β-actin
IgG
IP: α-Dbf4
B
H1299
R175Hp53
Vector 100 250 500 ng
Vector 100 250 500
IB: α-Cdc7
IgG HC
IB: α-Dbf4
C
H1299
R273Hp53
Vector 100 250 500 ng
Vector 100 250 500
D
SW480
shRNA Ctrl p53
shRNA Ctrl p53 Ctrl p53
E
H1299
EV EV R175H R273H
p-Mcm2
IgG
IP: Dbf4

Figure 4.

Figure 4. Increased level of Cdc7-Dbf4 kinase complex in cancer cells harboring GOF mutant p53.

A 500 μg of protein extracts from control and mutant p53-expressing H1299 stable cells were subjected to immunoprecipitation using anti-Dbf4 antibody or control rabbit serum IgG. Cdc7, Dbf4, and mutant p53 levels were evaluated in input fractions by Western blotting (left panel). Dbf4 immunoprecipitates were subjected to immunoblotting using anti-Cdc7, anti-Dbf4, anti-p53, and anti-β-actin antibodies (right panel).

B, C Co-immunoprecipitation assays showing relative amount of Cdc7-Dbf4 complex recovered from H1299 cells ectopically expressing mutant p53-R175H (B) and mutant p53-R273H (C). 500 μg of protein extracts from cells transfected with an increasing concentration of pCMV-R175Hp53 and pCMV-R273Hp53 was subjected to immunoprecipitation with anti-Dbf4 antibody or control rabbit serum IgG, 48 h post-transfection. Levels of Cdc7, Dbf4, and mutant p53 were evaluated in input fractions by Western blotting (left panel). Cdc7 and Dbf4 subunits in the immunoprecipitated fraction were detected by Western blotting using anti-Cdc7 and anti-Dbf4 antibodies (right panel).

D Co-immunoprecipitation assay showing relative amount of Cdc7-Dbf4 complex recovered from control and mutant p53-knocked down SW480 stable cells. The experiment was performed as described in (A). Levels of mutant p53 along with Cdc7 and Dbf4 upon mutant p53 knockdown were checked in input fraction by immunoblotting (left panel). Levels of Cdc7 and Dbf4 in immunoprecipitated fractions were determined by Western blotting using anti-Cdc7 and anti-Dbf4 antibodies (right panel).

E Autoradiograph showing the relative incorporation of ^{32}P in GST-Mcm2 N-terminal peptide incubated with active Cdc7 kinase complexes immunoprecipitated from control and mutant p53-expressing H1299 cells. Immunoprecipitate with rabbit serum IgG was used as negative control.

Data information: β-actin was used as loading control. *Indicates the specific bands. IgG heavy chains (IgG HC) are shown.
Source data are available online for this figure.

the well-characterized physiological substrates of Cdc7 involved in replication initiation [21]. *In vitro*, activated Cdc7 kinase extensively phosphorylates the N-terminal tail of Mcm2 [22]. We immunoprecipitated active DDK complexes from control and mutant p53-expressing H1299 cells and performed *in vitro* kinase assay using GST-Mcm2 N-terminal fragment (9–294) as a substrate. Increased phosphorylation of recombinant Mcm2 peptide was detected in reactions incubated with DDK complexes immunoprecipitated from mutant p53-expressing cells than that from the control cells (Fig 4E and Appendix Fig S1F). Hyper-phosphorylation of Mcm2 peptide further suggests that mutant p53 cells maintain relatively higher level of active Cdc7 kinase complex. Next, we carried out subcellular protein fractionation and looked into the phosphorylation levels of chromatin-bound Mcm2 in control and mutant p53-expressing H1299 cells. Along with higher amount of Cdc7 and Dbf4, we observed increased levels of Mcm2 phosphorylated at Cdc7-specific sites (Ser-53 and Ser-40) in nuclear soluble fractions as well as in chromatin-enriched fraction in mutant p53-expressing H1299 stable cells, thereby suggesting an enhanced activity of Cdc7 in these cells (Fig 5A). Cdc7-dependent phosphorylation of Mcm proteins facilitates the recruitment of crucial initiation factor Cdc45 to replication origins, which in turn promotes origin activation and DNA unwinding [13,23]. Importantly, compared to control cells, increased chromatin recruitment of Cdc45 was observed in GOF mutant p53 cells (Fig 5A). In agreement with these data, ectopic expression of mutant p53-R273H and p53-R175H resulted in increased chromatin recruitment of Cdc7, Dbf4, phosphorylated Mcm2, and Cdc45 in these cells (Fig 5B and C, respectively). Moreover, chromatin recruitment of Cdc7 and Dbf4 along with phosphorylated Mcm2 and Cdc45 was found to be decreased upon mutant p53 knockdown in SW480 cells (Fig 5D). Thus, chromatin enrichment of crucial replication initiation factors, including phosphorylated Mcm2 and Cdc45, suggests increased origin activation in cancer cells harboring GOF mutant p53.

Cdc7-dependent increased origin firing in GOF mutant p53 cells

Given the increased Cdc7 activity together with higher chromatin recruitment of phosphorylated Mcm2 and Cdc45 in GOF mutant p53 cells, we next compared the pattern of DNA replication initiation between control and mutant p53-expressing H1299 cells with or without *CDC7* knockdown using DNA fiber assay (Fig 6A and B). Compared to the control cells, we observed significantly higher percentage of newly fired origins in mutant p53-expressing cells (Fig 6C), thereby suggesting increased replication initiation in presence of GOF mutant p53. Further, partial knockdown of *CDC7* by tet-regulated shRNA (Fig EV3A) significantly rescued the elevated origin firing events back to control levels (Fig 6C). These results suggest Cdc7-dependent increased origin usage by cancer cells harboring mutant p53. Since increased origin firing frequency can inversely affect replication fork progression [24,25], we subsequently determined the fork speed by measuring the length of ongoing replication tracts (red-green) in these cells (Fig EV3B). Although origin firing was increased, no significant change in average fork speed was observed between control and p53-R175H-expressing cells (Fig 6D). When we inhibited excess origin firing by knocking down *CDC7*, these cells exhibited a small but significant increase in average fork speed (Fig 6D). This was also reflected in the fork speed distribution pattern (Fig 6E). This is in agreement with the notion that decrease in origin firing can promote replication fork progression [24]. However, compared to the control vector-infected cells, we found a significant decrease in average fork speed in p53-R273H-expressing cells (Fig 6D). The percentage of small forks (fork speed range, 0.4–0.99 kb/min) in p53-R273H-expressing cells was higher than that in control cells (Fig 6E). Given the maximum increase in origin firing frequency in cells expressing p53-R273H, reduced fork speed could be the compensatory consequence to maintain optimal replication dynamics in these cells. This was further supported by the restoration of fork speed upon inhibition of origin firing by *CDC7* knockdown (Fig 6D and E). In control H1299 cells, knockdown of *CDC7* resulted in decreased origin firing (Fig 6C) and subsequent increase in fork speed (Fig 6D and E). Together, these observations suggest that at molecular level, replication fork progression rate can be modulated by the degree of stochastic origin firing events or fork density under particular cellular conditions. We further investigated whether our observations from DNA fiber experiment correlate with the pattern of S-phase progression in cells harboring mutant p53. To this end, we compared the rate of S-phase progression between G1/S synchronized control and mutant p53-R175H-expressing H1299 stable cells with or without *CDC7* knockdown (Fig EV3C, D and E). We reasoned, since an increased level of origin firing with unaltered fork speed was observed in mutant p53-R175H-expressing cells,

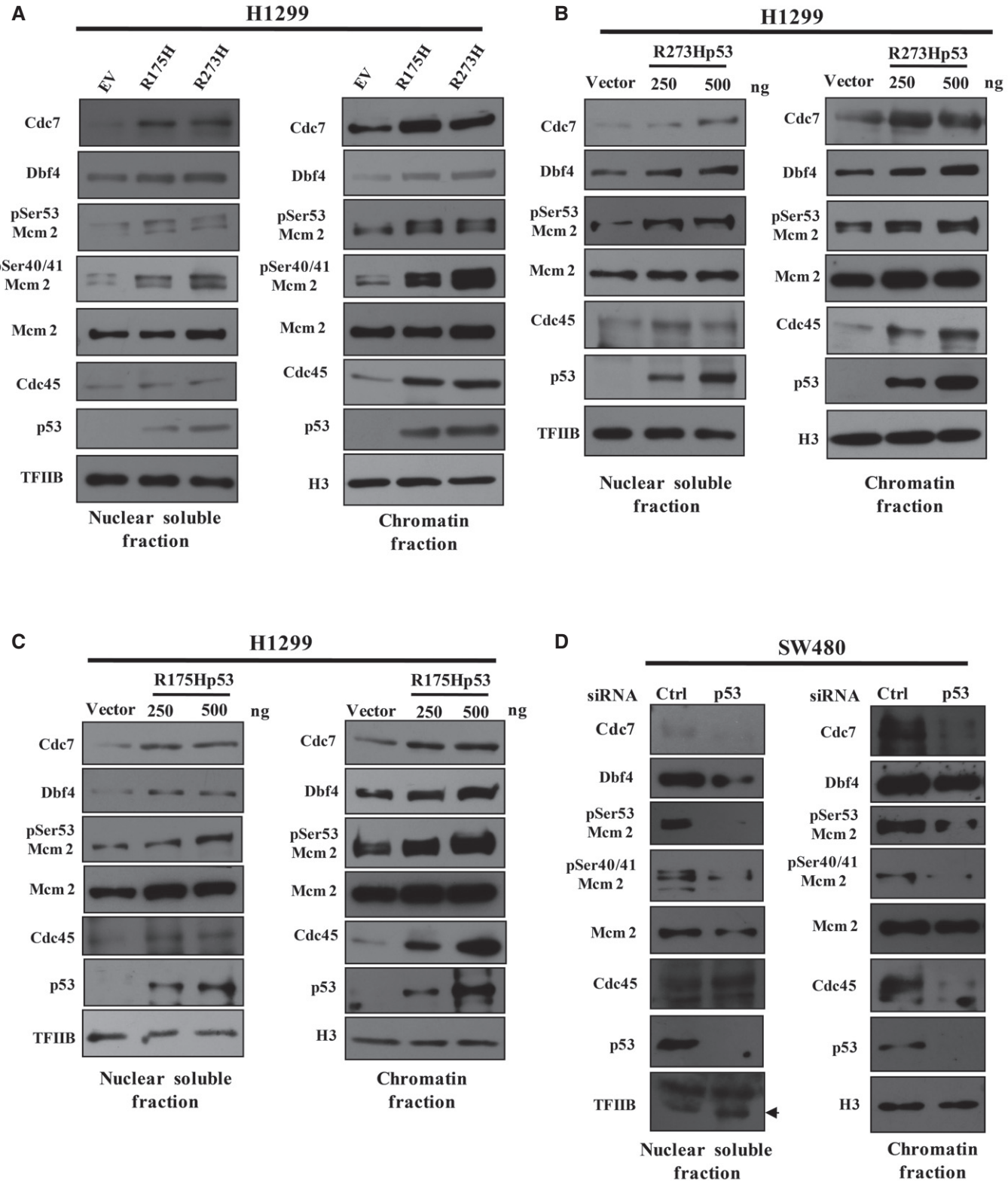

Figure 5.

these cells might exit S-phase earlier than the control cells. Cell cycle profile showed relatively faster S-phase progression in mutant p53-R175H-expressing cells (Fig 6F and Appendix Table S1). At 5 h after release from thymidine, when control (EV) cells showed a ratio of ~39% S/42% G2/M, mutant p53 cells showed a ratio of 28% S/54% G2/M, suggesting faster S transverse (Fig 6F and Appendix Table S1).

Figure 5. Chromatin enrichment of phosphorylated Mcm2 and Cdc45 in GOF mutant p53 cells.

A Control and mutant p53-expressing stable H1299 cells were subjected to biochemical fractionation. Nuclear soluble fraction and chromatin-enriched fraction were analyzed by immunoblotting using indicated antibodies.

B, C H1299 cells were transfected with increasing concentrations of mutant p53-R273H (B) and mutant p53-R175H (C). 48 h post-transfection, cells were harvested and subjected to biochemical fractionation.

D SW480 cells were transfected with 80 nM of either control siRNA or *TP53* siRNA, harvested after 72 h, and subjected to subcellular fractionation. The arrowhead points to the specific band.

Data information: TFIIB and histone (H3) were used as loading controls for nuclear soluble and chromatin-enriched fractions, respectively.
Source data are available online for this figure.

Further, partial knockdown of *CDC7* (Fig EV3C) did not rescue the S-phase length back to control level (Fig 6F and Appendix Table S1), which can be logically explained by the compensatory small but significant increase in fork speed for reduced replication initiation in mutant p53-R175H-expressing cells upon partial *CDC7* knockdown (Fig 6D). Similar results were obtained when we monitored the progression of these cells through S-phase using BrdU pulse chase assay (Fig EV4). Partial depletion of *CDC7* (Fig EV3C) did not decelerate S-phase also in control EV cells (Fig 6F and Appendix Table S1). Overall these data are in agreement with the results obtained from the DNA fiber analyses and suggest that it is the level of origin firing and associated replication fork speed that determines the replication-timing program and length of S-phase.

Cdc7 knockdown attenuates oncogenic properties of GOF mutant p53-bearing cancer cells

A number of previous studies evidenced higher activation of replication origins in tumor cells, thereby suggesting increased origin firing as a critical molecular event during the evolution of cancer cells [10,26]. Since mutant p53-expressing cells showed Cdc7-dependent increased replication initiation, we investigated the potential contribution of Cdc7 in mutant p53-driven cancer phenotypes. First, we examined the effect of *CDC7* knockdown on clonogenic potential of control null or wild-type and GOF mutant p53-expressing H1299 cells by colony formation assay (Fig 7A). In order to avoid the possible effect of clonal variability on *CDC7* knockdown level and the subsequent outcome of the assay, we transfected H1299/control shRNA or H1299/*CDC7* shRNA cells with empty vector, wild-type and mutant p53-encoding plasmids and generated stable cells by G418 selection. As expected, cells expressing mutant p53 formed significantly higher number of colonies than control cells, whereas wild-type p53 inhibited colony formation (Fig 7A). Importantly, knockdown of *CDC7* reduced the increased colony-forming ability of mutant p53 cells (Fig 7A). Since Cdc7 is a key component of replication machinery and essential for cell growth, knockdown of *CDC7* also reduced the colony-forming ability of control null cells, albeit to lesser extent (average colony number reduced by 60 and 80% in control and mutant p53-expressing cells, respectively, upon *CDC7* knockdown) than cells harboring mutant p53 (Fig 7A). In wild-type p53-bearing cells, no significant difference in clonogenicity was observed upon *CDC7* knockdown (Fig 7A). Using soft agar anchorage-independent growth assay, we further investigated the possible contribution of Cdc7 to enhanced tumorigenic potential of mutant p53 cancer cells (Fig 7B). Compared to the control cells, mutant p53 cells formed higher number of colonies on soft agar (Fig 7B). Notably, knockdown of *CDC7* significantly inhibited this growth-promoting effect of p53 mutants (Fig 7B). These results suggest that Cdc7 contributes to enhanced tumorigenicity conferred by GOF mutant p53. It may be noted, however, that in most of the experiments knockdown of *CDC7* was partial as reflected in the respective immunoblots. Enhanced chemoresistance is a well-characterized phenotype of cancer cells harboring mutant p53 [5,27–29]. As Cdc7 plays an important role in DNA damage bypass pathway [14], we tested whether perturbation of *CDC7* expression could reverse the increased chemoresistance phenotype of mutant p53 cells. Partial knockdown of *CDC7* significantly increased the sensitivity of mutant p53-expressing H1299 cells to cisplatin (Fig 7C). In contrast, no significant increase in cisplatin sensitivity was observed in control H1299 cells harboring empty vector alone (Fig 7D). However, since wild-type p53 cells are generally drug-sensitive in nature, partial depletion of *CDC7* had much less effect on cisplatin sensitivity in H1299/WTp53 cells (Fig 7D). Partial knockdown of *CDC7* in SkBr3 and SW480 cells harboring endogenous mutant p53 also resulted in a significant decrease in cell survival from 5-FU treatment (Fig 7E). We further validated our cell-based observations in mouse xenograft model. H1299/EV and H1299/mtp53^{R175H} cells harboring doxycycline-inducible control or *CDC7* shRNA were introduced in NOD/SCID mice and allowed to form subcutaneous tumor (Fig EV5A). Mutant p53 clearly promoted the growth of H1299 xenograft tumors (Fig 8A and B). Further, knockdown of *CDC7* significantly attenuated this growth-promoting effect of mutant p53 *in vivo* (Fig 8A and B). In order to investigate the effect of *CDC7* knockdown on acquired chemoresistance phenotype of mutant p53 cancer cells *in vivo*, we examined 5-FU sensitivity of xenograft tumors generated from SW480 cells harboring either control or *CDC7* shRNA (Fig EV5D). As expected, tumors generated from SW480 cells bearing control shRNA showed resistance to 5-FU treatment (Fig 8C and D). Notably, compared to the 5-FU-treated control tumors, volume and weight of *CDC7*-knocked down tumors were significantly (P-value = 0.0133) reduced upon 5-FU treatment (Fig 8C and D). Although not statistically significant (P-value = 0.0867), weight of the *CDC7*-knocked down tumors was also found to be reduced in response to 5-FU (Fig 8D). RT–qPCR and immunohistochemical analysis of xenograft tumor specimens confirmed doxycycline-induced *in vivo* partial knockdown of *CDC7* under our standard experimental conditions (Fig EV5B, C, E and F). Collectively, these results suggest that Cdc7 inhibition can be an efficient strategy to target GOF p53 tumors.

High *CDC7* expression correlates with poor prognosis in lung adenocarcinoma patients

We investigated the clinical significance of *CDC7* expression in lung adenocarcinoma patients by analyzing TCGA lung adenocarcinoma

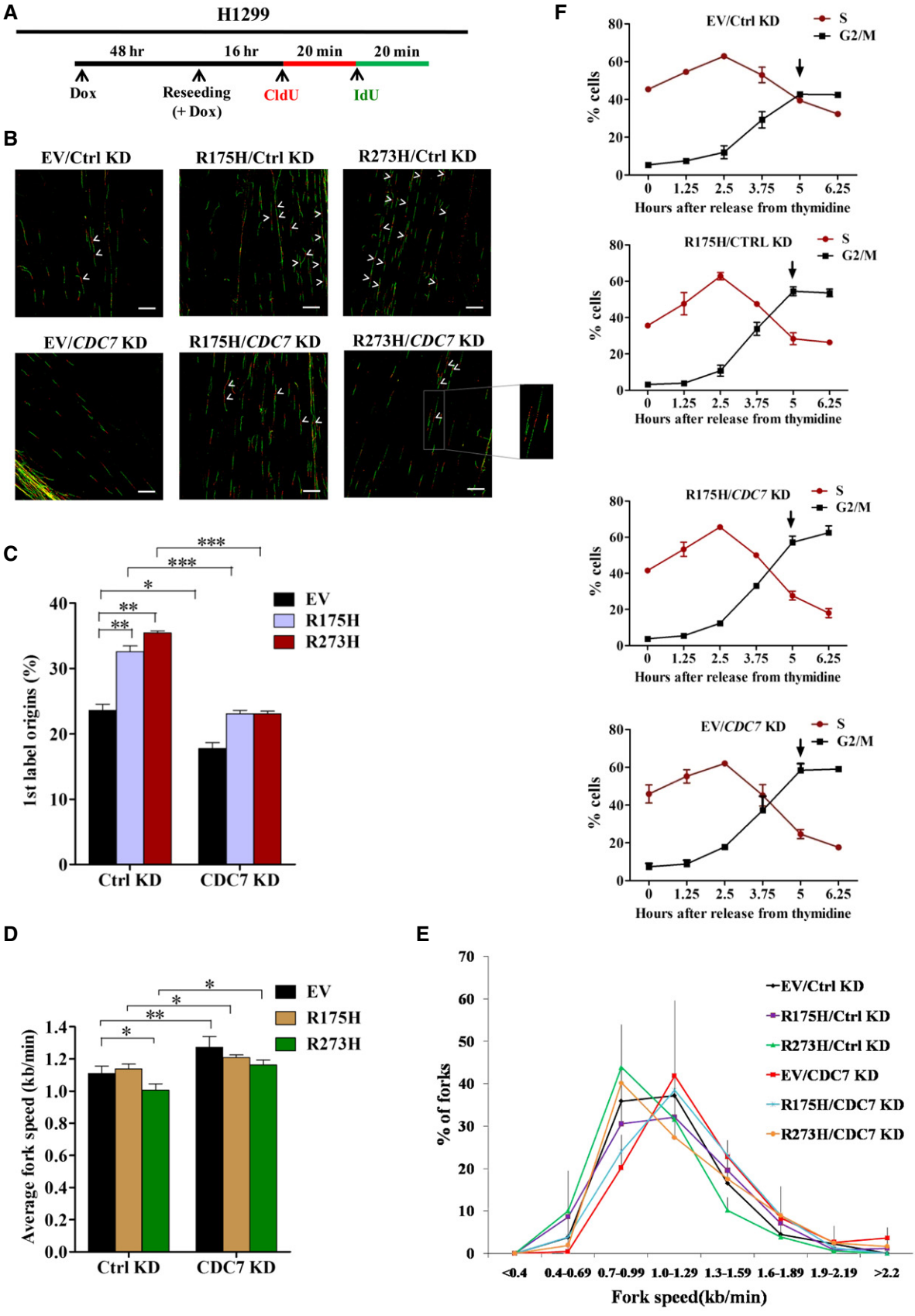
A
H1299
48 hr
16 hr
20 min
20 min
Dox
Reseeding (+ Dox)
CldU
IdU
B
EV/Ctrl KD
R175H/Ctrl KD
R273H/Ctrl KD
EV/CDC7 KD
R175H/CDC7 KD
R273H/CDC7 KD
C
1st label origins (%)
EV
R175H
R273H
Ctrl KD
CDC7 KD
D
Average fork speed (kb/min)
EV
R175H
R273H
Ctrl KD
CDC7 KD
E
% of forks
EV/Ctrl KD
R175H/Ctrl KD
R273H/Ctrl KD
EV/CDC7 KD
R175H/CDC7 KD
R273H/CDC7 KD
<0.4
0.4-0.69
0.7-0.99
1.0-1.29
1.3-1.59
1.6-1.89
1.9-2.19
>2.2
Fork speed(kb/min)
F
EV/Ctrl KD
R175H/CTRL KD
R175H/CDC7 KD
EV/CDC7 KD
S
G2/M
% cells
Hours after release from thymidine

Figure 6.

Figure 6. Cdc7-dependent increased origin firing in GOF mutant p53 cells.

A Schematic representation of the DNA fiber assay. Asynchronously growing control and mutant p53-expressing H1299 stable cells harboring either control or *CDC7* shRNA were treated with doxycycline (DOX) to induce the expression of the respective shRNAs. After 48 h, cells were trypsinized and ~0.1 × 10^6 cells were reseeded in each well of six-well plates. Cells were grown for another 16 h in presence of doxycycline followed by sequential labeling with CldU and IdU.

B Representative images of CldU- and IdU-labeled DNA tracts obtained from the fiber assay. Arrowheads indicate 1st label bidirectional origins (green-red-green). A bidirectional origin structure is shown in inset. Scale bars represent 20 μm.

C Quantification of origin firing frequency from fiber assay data. Origin firing was measured as the percentage of 1st label origin structures (green-red-green) among the total red label (CldU) fibers.

D Bar graphs showing average fork speeds in cells described in (A).

E Line graphs showing percentage of ongoing forks distributed over the range of fork speed in individual cells.

F S-phase progression rate of control and mutant p53-R175H-expressing H1299 stable cells with or without *CDC7* knockdown. Cells were synchronized at G1/S using double-thymidine block, and cell cycle profiles were analyzed by FACS. The change in percentage of S (red line)- and G2/M (black line)-phase cells over time is shown. Arrows indicate the relative percentage of S and G2/M phase cells at 5 h time point in individual sample.

Data information: Data represent mean ± SD; $n = 3$; two-tailed Student's *t*-test: $^*P < 0.05$, $^{**}P < 0.01$, $^{***}P < 0.001$.
Source data are available online for this figure.

cohort (Dataset EV3). Patients with high *CDC7* expression (> 50th percentile) showed significantly reduced overall survival (OS) than those with low *CDC7* expression (≤ 50th percentile), suggesting *CDC7* expression as a critical determinant of lung cancer patients' survival (Fig 8E, left panel). Importantly, we found that majority of the patients with high *CDC7* expression harbored mutant p53, whereas patients with low *CDC7* expression were predominantly of wild-type p53 status (Dataset EV3 and Fig 8E, right panel). These data further suggest that p53 mutation is correlated with high *CDC7* expression in lung cancer patients. To further strengthen our findings, we next compared the overall survival of patients with high (> 75th percentile), intermediate (75th–25th percentile), and low (< 25th percentile) *CDC7* expression (Appendix Fig S2). We found a significant OS trend between these three groups of patients in which patients' survival decreases with high levels of *CDC7* (Appendix Fig S2, left panel). In accordance, the number of patients with wild-type and mutant p53 was significantly different between these three groups of patients (Appendix Fig S2, right panel). Further, in an attempt to understand whether poor survival is simply caused by high *CDC7* expression, by p53 mutation or by the combination of both, we examined the relative survival of patients harboring wild-type and mutant p53 with high or low *CDC7* expression (Fig 8F). High *CDC7* expression predicted poor survival in both wild-type and mutant p53 patients, whereas p53 mutation alone could not show any effect on patients' survival (Fig 8F). Our analyses suggest that high *CDC7* expression determines poor prognosis in lung adenocarcinoma patients irrespective of their *TP53* status. Further, multivariate Cox regression analysis showed that *CDC7* expression is an independent prognostic factor of overall survival in lung adenocarcinoma patients (Fig 8G).

Discussion

Gain-of-function (GOF) mutant p53 promotes several oncogenic phenotypes by modulating diverse cellular genes and pathways [30]. Though a couple of recent reports provided clues about the regulation of replication pathway by mutant p53, the particular area is much unexplored [7,31]. In this study, we delineated the role of GOF mutant p53 in regulating replication initiation in cancer cells. Pathway enrichment analysis revealed DNA replication as the most over-represented pathway targeted by GOF mutant p53 in lung adenocarcinoma patients. As reported earlier in triple-negative breast cancer (TNBC), we did not observe proteasome pathway as a highly enriched target of GOF mutant p53, probably due to the difference in tumor types [6]. We showed that replication initiation factor Cdc7 kinase is upregulated by GOF mutant p53 in NSCLC cells. Although we found a subtle change in Cdc7 expression, a biologically significant effect of this regulation was observed on replication initiation process in GOF mutant p53 cells. Since undue overexpression of Cdc7 can lead to S-phase arrest due to excessive origin firing [32], our observations suggest that mutant p53 may influence Cdc7 expression at an optimum level sufficient to induce origin firing without impeding cell proliferation or viability. On the other hand, in accordance with the previous reports, our data suggest that wild-type p53 can transcriptionally repress *CDC7* [33,34]. However, we did not observe recruitment of wild-type p53 on *CDC7* promoter in ChIP assay, suggesting an indirect mechanism of transcriptional repression. Transcriptional regulation of different genes involved in signal transduction underlies the gain-of-function properties of mutant p53 [2,35,36]. Given the loss of sequence-specific DNA binding property, previous studies identified crucial TFs that interact with and recruit mutant p53 onto the promoters of their respective target genes. Here, we provide evidence that GOF mutant p53 transactivates *CDC7* through Myb, an oncogenic transcription factor [37]. We report that p53 mutants directly interact with Myb *in vivo*. Consistent with the previous reports, wild-type p53 was also found to interact with Myb [17,18]. Furthermore, our experimental results indicate that the C-terminal tetramerization domain of mutant p53 might be responsible for interaction with Myb. It is worth noting that wild-type p53 has been reported to interact with Myb also via the tetramerization domain and this domain is required for mutant p53 to interact with other transcriptional regulators including ETS2 and YAP [18–20]. Experimental results also suggest that Myb is critical for recruitment of mutant p53 to *CDC7* promoter and the subsequent transactivation of the gene, although we cannot rule out the involvement of other mechanisms.

Along with increased *CDC7* expression, we observed a concomitant increase in Dbf4 protein level without any significant change in the transcript amount in mutant p53-expressing cells. It has been previously reported that mutant p53 can increase the level of replication initiation proteins including PCNA and MCM4 without changing their respective transcript abundance [7]. Dbf4 is among the cell cycle proteins targeted for degradation by APC/C^{Cdh1} in late mitosis and has been reported to get stabilized via

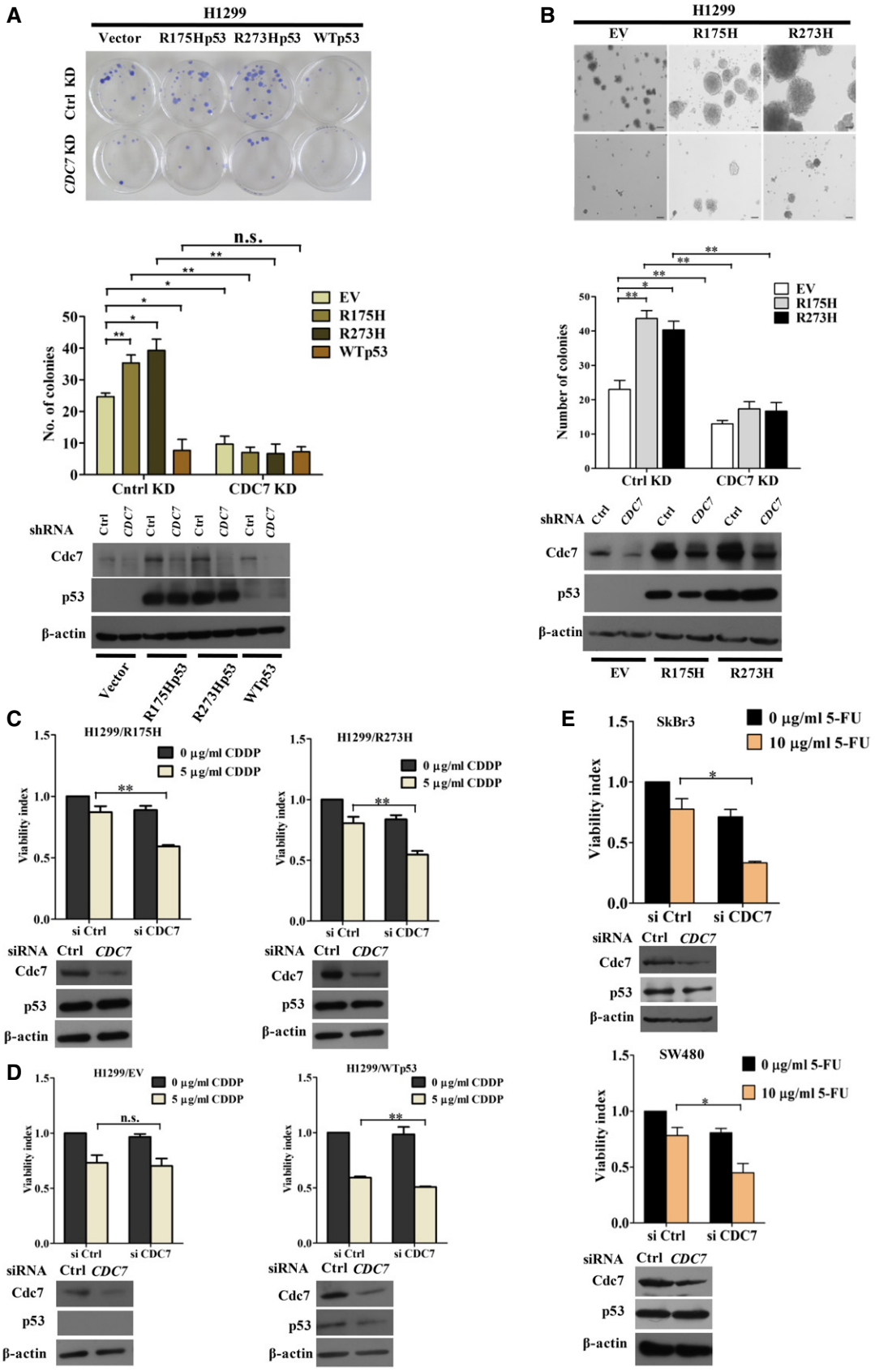
A
H1299
Vector
R175Hp53
R273Hp53
WTp53
Ctrl KD
CDC7 KD
n.s.
EV
R175H
R273H
WTp53
No. of colonies
Cntrl KD
CDC7 KD
shRNA
Ctrl
CDC7
Cdc7
p53
β-actin
B
H1299
EV
R175H
R273H
Number of colonies
Ctrl KD
CDC7 KD
C
H1299/R175H
H1299/R273H
0 μg/ml CDDP
5 μg/ml CDDP
Viability index
si Ctrl
si CDC7
siRNA
D
H1299/EV
H1299/WTp53
n.s.
E
SkBr3
SW480
0 μg/ml 5-FU
10 μg/ml 5-FU

Figure 7.

Figure 7. *CDC7* knockdown reduces oncogenic phenotypes of GOF mutant p53 cells.

A (Upper panel) Representative images of colonies formed by control H1299/EV, H1299/R175Hp53, H1299/R273Hp53, and H1299/WTp53 cells harboring either control or *CDC7* shRNA in clonogenic assay. Cells were treated with doxycycline (1 μg/ml) for 48 h, plated on 6-cm dishes (~1,500 cells), and allowed to grow in presence of doxycycline (0.25 μg/ml) until the colonies appear. Colonies were stained with 0.1% methylene blue and counted. (Middle panel) Bar graphs showing number of colonies formed by the respective cells. (Lower panel) Immunoblots showing the levels of Cdc7 and p53 in cells seeded in parallel to evaluate *CDC7* knockdown level upon doxycycline treatment.

B (Upper panel) Representative images of colonies formed on soft agar by control (EV) and mutant p53-expressing H1299 cells. Cells (~2,000) were grown on soft agar in presence of doxycycline (0.25 μg/ml) for 2–3 weeks, and the number of visible colonies was counted. Scale bar represents 50 μm. (Middle panel) Quantification of the data obtained from soft agar assay. (Lower panel) Immunoblots showing *CDC7* knockdown level upon doxycycline treatment.

C Bar graphs showing relative viability index of cisplatin (CDDP)-treated H1299/R175H (left panel) and H1299/R273H (right panel) stable cells upon siRNA-mediated knockdown of *CDC7*. Knockdown of *CDC7* was assessed by Western blotting.

D Relative viability of control H1299/EV (left panel) and H1299/WTp53 (right panel) cells upon *CDC7* knockdown. The levels of *CDC7* knockdown were assessed by Western blotting.

E Bar graphs showing relative 5-FU sensitivity of SkBr3 (upper panel) and SW480 (lower panel) cells upon *CDC7* knockdown. Immunoblots showing the *CDC7* knockdown levels.

Data information: β-actin was used as loading control. Data represent mean ± SD of three independent experiments. Two-tailed Student's *t*-test: $*P < 0.05$, $**P < 0.01$; n.s., non-significant.
Source data are available online for this figure.

ATR–Chk1–APC/C^{Cdh1} pathway under replication stress in order to prevent replication collapse [14,38]. Since oncogenes induce replication stress leading to checkpoint activation, increased level of Dbf4 protein in mutant p53-expressing cells might be attributed to increased stabilization of the protein [39]. Accordingly, higher amount of active DDK complex was also detected in mutant p53-expressing cells, suggesting increased Cdc7 activity in presence of mutant p53. This was further supported by increased chromatin recruitment of phosphorylated Mcm2 in mutant p53 cells. Cdc7-dependent chromatin recruitment of replication initiation factor Cdc45 is crucial for pre-initiation complex (pre-IC) formation and subsequent activation of individual replication origins [13,23]. Earlier reports also suggest that increased on-chromatin recruitment of Cdc45 is an important marker for increased origin usage by cells [40,41]. We observed increased level of chromatin-bound Cdc45 in mutant p53-expressing cells, thereby suggesting increased replication initiation in cells with GOF mutant p53. We present further evidence in support of this hypothesis by looking into the replication dynamics of GOF mutant p53 cells. Using DNA fiber assay, we showed that replication origin firing was increased in cells expressing GOF mutant p53. Furthermore, restoration of increased origin firing to control level upon *CDC7* knockdown suggests that the effect is Cdc7 dependent. Increased origin firing can lead to slow fork progression, most likely due to the excess utilization of nucleotide pool [24,25]. However, in spite of the increased level of origin firing, fork speed was unaffected in H1299 cells expressing mutant p53-R175H. In contrast, H1299 cells harboring mutant p53-R273H showed a significant decrease in fork progression rate compared to the control cells. The probable interpretation for this observation could be that fork speed was decreased in order to compensate for the excessive origin firing in presence of p53-R273H. Together, these observations suggest that it is the level of origin usage that determines fork speed under a particular condition. Further, in order to interrogate the possible effects of mutant p53-induced altered replication on S-phase progression, we compared the length of S-phase between control and mutant p53-R175H-expressing H1299 cells. Although fork speed was unaffected, mutant p53-expressing cells completed S-phase faster than control cells, suggesting that firing of more number of origins may facilitate early completion of S-phase [42]. However, inhibition of origin firing by partial *CDC7* knockdown did not slow down S-phase progression either in mutant p53-expressing cells or in control p53 null cells, which was likely due to the compensatory increase in fork speed upon *CDC7* depletion, as reported previously [24].

Figure 8. *CDC7* Knockdown attenuates mutant p53 GOF phenotypes *in vivo* and high *CDC7* expression correlates with poor survival in lung adenocarcinoma patients.

A Line graph showing the relative growth rate of xenograft tumors generated from control and mutant $p53^{R175H}$-expressing H1299 cells harboring either control or *CDC7* shRNA. Data represent mean ± SEM ($n = 5$). *P*-values were determined by two-tailed Student's *t*-test.

B Bar graph showing relative weight (mg) of the tumors described in (A). Data represent mean ± SEM. *P*-values were determined by two-tailed Student's *t*-test.

C Line graph showing relative growth rate of tumors in response to 5-FU treatment in SW480 cells harboring either control or *CDC7* shRNA. Once tumors reached a palpable size, mice were injected with either DPBS or 5-FU (10 mg/kg) intraperitoneally and after 10 successive treatment, change in tumor volume was measured at regular interval up to 20 days. Data represent mean ± SEM ($n = 4$). *P*-values were calculated by two-tailed Student's *t*-test.

D Bar graph showing relative weight (mg) of the tumors excised from SW480 xenografts after 20 days of drug treatment. Data represent mean ± SEM ($n = 4$). *P*-values were determined by two-tailed Student's *t*-test. n.s., non-significant.

E (Left panel) Overall survival probabilities of TCGA lung adenocarcinoma patients with high and low *CDC7* expression (50^{th} percentile) estimated by Kaplan–Meier analysis. *P*-value was calculated using log-rank (Mantel–Cox) test. Median survival time and number of patients at risk are shown. (Right panel) Bar graphs showing relative distribution of patients with wild-type and mutant p53 in high and low *CDC7*-expressing groups. *P*-value was calculated using Fisher's exact test.

F Relative survival of patients harboring wild-type and mutant p53 with high or low *CDC7* expression. Median survival time for each group of patients is shown.

G Multivariate Cox regression analysis showing *CDC7* expression as a significant independent predictor of poor survival in lung adenocarcinoma patients. Significant *P*-values (< 0.05) are shown in bold.

Source data are available online for this figure.

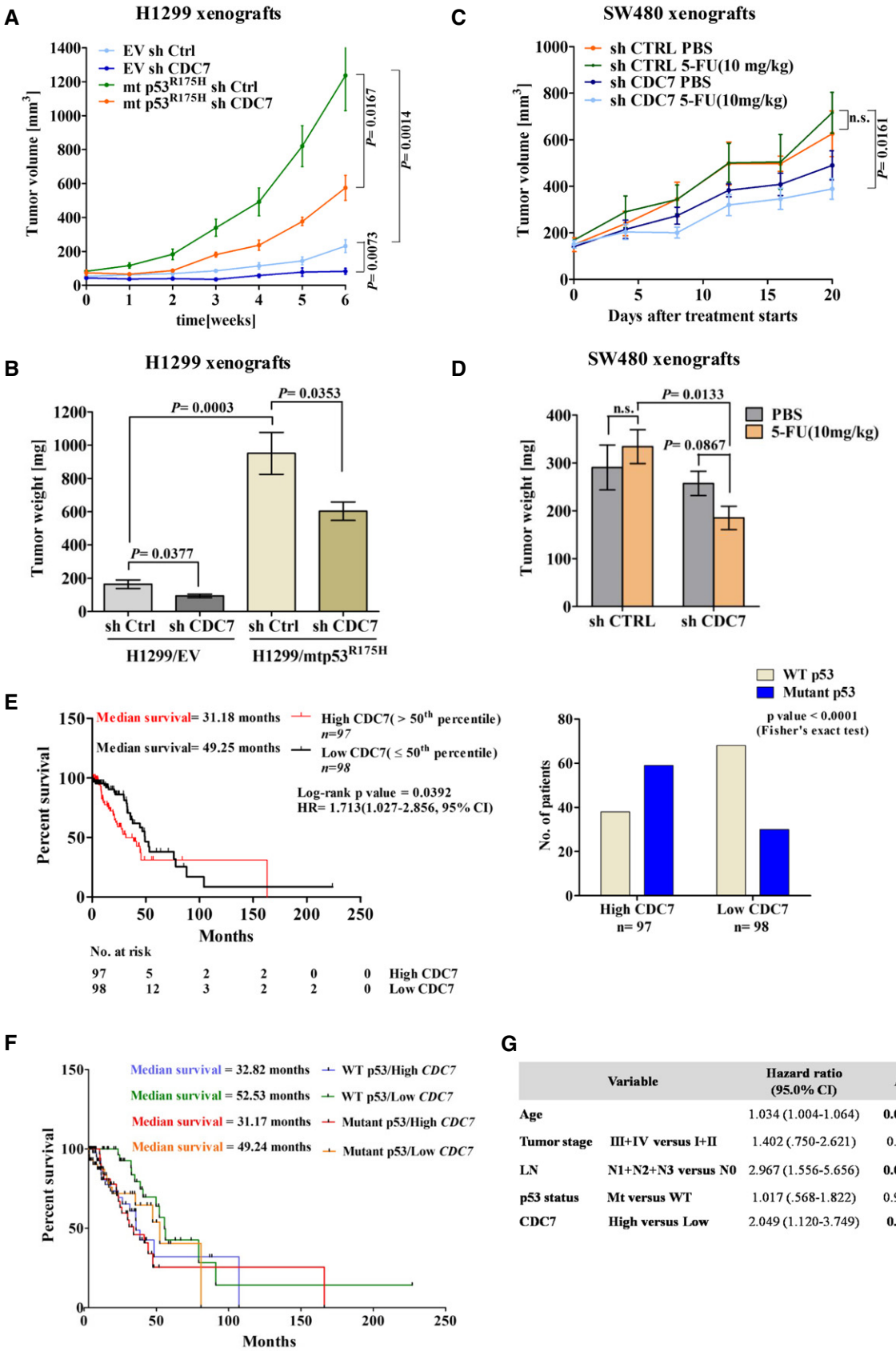

G

Variable		Hazard ratio (95.0% CI)	P
Age		1.034 (1.004-1.064)	**0.026**
Tumor stage	III+IV versus I+II	1.402 (.750-2.621)	0.29
LN	N1+N2+N3 versus N0	2.967 (1.556-5.656)	**0.001**
p53 status	Mt versus WT	1.017 (.568-1.822)	0.955
CDC7	High versus Low	2.049 (1.120-3.749)	**0.02**

Figure 8.

Perturbation of Cdc7 activity has been reported to induce apoptotic cell death in some cancer cell types and restrains tumor growth in preclinical mouse models [15,43]. On the other hand, normal cells simply become arrested in response to Cdc7 depletion instead of cell death; thus, Cdc7 inhibition has become an attractive strategy for targeted cancer therapy [15,43,44]. We found that NSCLC cells harboring GOF mutant p53 lose increased clonogenic competence upon partial depletion of *CDC7* in cultured cells. Moreover, *in vivo* partial knockdown of *CDC7* retarded tumor growth of NSCLC cells harboring GOF mutant p53. These observations suggest that Cdc7-dependent increased replication initiation contributes to enhanced tumorigenic potential of mutant p53 cells. Further, we show that *CDC7* knockdown attenuates enhanced chemoresistance property of mutant p53 cells both *in vitro* and *in vivo*. Given the critical role of Cdc7 under replication stress and DNA damage response [14], we hypothesize that increased Cdc7 activity and subsequent increase in replication initiation empowers GOF mutant p53 cells to withstand the effect of DNA damage caused by the conventional chemotherapeutics. Since tumors with mutant p53 are highly chemoresistant in nature, our observations suggest that selective perturbations of DNA replication pathway might be an effective strategy to overcome the barrier. Finally, our analyses show *CDC7* expression as a significant predictor of clinical outcomes in lung adenocarcinoma patients predominantly of mutant p53 status. In conclusion, the present study provides mechanistic insights into the emerging role of GOF mutant p53 in regulating DNA replication in cancer cells. We propose Cdc7-dependent altered replication initiation as an important factor in mutant p53-driven oncogenesis. It would be interesting to see whether or not the effect on DNA replication is a universal gain-of-function property of mutant p53.

Materials and Methods

Cell culture, plasmids, and transfection

H1299-EV and H1299-R175H were kindly provided by Prof. Varda Rotter (Weizmann Institute of Science, Rehovot, Israel) and were cultured in RPMI-1640 medium (Gibco) [45]. H1299-R273H stable cell line was generated by stable transfection of basic H1299 cell line (provided by Dr. Tanya Das, Bose Institute, India) with pCMV-Neo-Bam-p53-R273H (provided by Dr. Bert Vogelstein, Johns Hopkins Kimmel Cancer Center, MD, USA) using Lipofectamine 2000 (Invitrogen) followed by gradual selection with G418 (800 μg/ml, Gibco). To ensure that the H1299 stable cells used in this study were of same parental background, H1299/EV, H1299/mtp53R175H, and H1299/mtp53R273H cell lines were authenticated by STR profiling (CellSure-Human, Lifecode Technologies). SW480 and SkBr3 cell lines were obtained from ATCC. HCT116 $p53^{-/-}$ cell line was gifted by Prof. Bert Vogelstein. These cell lines were cultured in Dulbecco's modified Eagle's medium (DMEM, Gibco) supplemented with 10% fetal calf serum, 1% Pen Strep and 0.006% Gentamicin (Gibco). GIPZ *TP53* (RHS5086-EG7157) and TRIPZ *CDC7* (RHS5087-EG8317) Lentiviral shRNAs were purchased from GE Dharmacon. Lentiviral particles produced were used to infect target cells following manufacturer's protocol. Stable transduced cells were selected by puromycin (Gibco) and knockdown efficiencies were verified by Western blotting. H1299 and HCT116 $p53^{-/-}$ cells were transiently transfected with pCMV-R175H and pCMV-R273H expression plasmids and harvested after 48 h for assessing *CDC7* expression. Cells were transfected with either non-targeting control pool (D-001810-10-05) or SMART pool siRNAs (GE Dharmacon) directed against *TP53* (L-003329-00-0005), *CDC7* (L-003234-00-0005) and *MYB* (L-003910-00-0005) at a final concentration of 80 nM using DharmaFECT 1 (GE Dharmacon) and harvested after 72 h. HA-tagged p53-R175H, p53-R175H Δproline, p53-R175H (1–338), p53-R175H (1–355), and p53-R175H (22,23) plasmids were kindly provided by Prof. Luis Alfonso Martinez, Stony Brook University, NY, USA. Myb cDNA clone was purchased from Origene (SC116779). pGEX6P expression plasmid encoding GST-tagged Mcm2 (9–294) was kindly provided by Prof. Corrado Santocanale, National University of Ireland, Galway, Ireland.

Real-time PCR

Total RNA from cell lines was isolated using TRIzol (Invitrogen). Xenograft tumor tissues were disrupted in TissueLyser LT (Qiagen) and RNA was isolated using RNeasy Plus Mini kit (Qiagen) following manufacturer's protocol. One microgram of RNA was reverse-transcribed using Verso cDNA synthesis kit (Thermo Scientific) following manufacturer's protocol. Quantitative PCR was performed in ABI 7500 Fast and StepOnePlus Real Time PCR platforms (Applied Biosystems) using Fast start universal SYBR Green master mix (#04913850001, Roche). β-actin or 18s rRNA was used as internal reference control. The fold changes were calculated using the formula $2^{-\Delta\Delta C_T}$. Primers used in real-time PCR are listed in Appendix Table S2.

Western blotting

Cells were lysed in NP-40 cell lysis buffer (FNN0021, Invitrogen) supplemented with protease and phosphatase inhibitor (#88669, Thermo Scientific). Equal amount of proteins were subjected to SDS–PAGE followed by immunoblotting with specific antibodies listed in Appendix Table S3. The protein bands were developed on autoradiography films using SuperSignal™ West Pico PLUS Chemiluminescent substrate (#34080, Thermo Scientific) and Luminata Forte Western HRP substrate (WBLUF0100, Merck Millipore).

Promoter cloning and luciferase reporter assay

CDC7 (−634/+82 and −383/+82 wrt TSS) and *DBF4* (−859/+102 wrt TSS) promoter regions were cloned into T/A cloning vector pTZ57R/T (Thermo Scientific) and sub-cloned in pGL3 basic vector (Promega) following manufacturer's protocol. Myb binding sites on *CDC7* promoter were mutated using QuikChange XL site-directed mutagenesis kit (#200517-5, Agilent Technologies) following manufacturer's protocol. Primers used for promoter cloning are listed in Appendix Table S2. Cells were co-transfected with 100 ng of promoter luciferase and 25 ng of control *Renilla* luciferase (pRL-TK, E2241, Promega) plasmids. In dose-dependent experiments, 100 ng of luciferase constructs were co-transfected either with pcDNA3.1 vector alone or with increasing concentrations of pCMV-R175H or pCMV-R273H plasmids in H1299 cells. After 48 h, luciferase assay was performed using dual-luciferase assay kit (E1910, Promega) following manufacturer's protocol. Relative luciferase activity was determined as a ratio of firefly/*Renilla* luminescence.

Chromatin immunoprecipitation (ChIP) assay

Cells grown in 10 cm dishes (~8 × 10^6 cells) were cross-linked in 1% formaldehyde (F8775, Sigma) containing medium for 10 min at 37°C followed by glycine quenching. Cells were lysed in lysis buffer supplemented with protease inhibitors and PMSF (P7626, Sigma) and sonicated in Bioruptor (Diagenode). Cell lysates diluted (1:5) with ChIP dilution buffer were pre-cleared using protein A Sepharose beads (P9424, Sigma) blocked with 3% BSA and salmon sperm DNA for 30 min at 4°C. Pre-cleared lysates were incubated with 10 μg of either specific antibodies or with rabbit serum IgG overnight at 4°C. The immune complexes were subsequently incubated with blocked protein A Sepharose beads for 1 h at 4°C. The protein A Sepharose/antibody/chromatin complexes were washed with low-salt, high-salt, LiCl, and Tris–EDTA buffers, respectively. The washed immunoprecipitated chromatin fractions were reverse cross-linked by adding Chelex 100 resin (# 1422822, Bio-Rad) followed by heating at 100°C. After Proteinase K (AM2548, Invitrogen) treatment, DNA was purified using phenol–chloroform. ChIP DNA was amplified using specific primer pairs by qPCR. Primer sequences, antibodies and composition of ChIP buffers are provided in Appendix Tables S2, S3, and S4 respectively.

Co-immunoprecipitation assay

Cells were lysed in NP-40 cell lysis buffer supplemented with protease inhibitors, and cell lysates were incubated with either specific antibodies (Appendix Table S3) or with rabbit serum IgG overnight at 4°C. The solutions were incubated with blocked (3% BSA) protein A Sepharose beads at 4°C for 1 h. The beads were stringently washed with lysis buffer, resuspended in 2× Laemmli buffer with β-mercaptoethanol and boiled at 95°C for 5 min. The immunoprecipitates were subjected to SDS–PAGE and blotted with specific antibodies listed in Appendix Table S3.

Purification of GST-Mcm2 and *in vitro* kinase assay

Expression of GST-Mcm2 peptide was induced at 20°C by the addition of 0.5 mM IPTG in log-phase *Escherichia coli* cells harboring pGEX6P-Mcm2. The clarified cell extracts were incubated with glutathione agarose resin (G-250-10, Gold Biotechnology) at 4°C for 3 h. Beads were washed extensively with lysis buffer, and GST-Mcm2 proteins were eluted with elution buffer. Kinase assay was performed as described previously with some modifications [46]. Active DDK complexes were immunoprecipitated with anti-Dbf4 antibody (H-300, sc-11354, Santa Cruz Biotechnology) from 500 μg of total protein extracts and subjected to kinase assay using GST-Mcm2 peptide (2 μg). The composition of buffers is provided in Appendix Table S4.

Subcellular protein fractionation

Cells (~3 × 10^6) were incubated in 300 μl of cytoplasmic extraction buffer at 4°C for 10 min with gentle shaking. Cell lysates were centrifuged at 500 × *g* at 4°C for 5 min, and 150 μl of nuclear extraction buffer was added to the pellet followed by vortexing and incubation at 4°C for 30 min with end-to-end rotation. After centrifugation at 5,000 × *g* for 5 min, supernatants containing nuclear soluble fractions were collected and the pellet was dissolved in 100 μl of chromatin extraction buffer by vigorous vortexing followed by incubation at 37°C for 15 min. After centrifugation at 15,000 × *g*, supernatants containing chromatin fractions were collected. The composition of buffers is provided in Appendix Table S4.

DNA fiber assay

DNA fiber experiment was performed as described previously with some modifications [31,47]. Exponentially dividing cells (~0.1 × 10^6) were sequentially labeled with 100 μM CldU (C6891, Sigma) and 250 μM IdU (I7125, Sigma) for 20 min each. The cells were trypsinized and counted, and 2,000 cells were spotted and lysed (200 mM Tris–HCl pH 7.4, 50 mM EDTA and 0.5% SDS) on silane-coated slides (S4651-72EA, Sigma). The slides were kept in tilted position to stretch the DNA fibers followed by air drying, fixation (methanol: acetic acid, 3:1) and incubation in 2.5 M HCl at RT for 1 h. Next, the slides were neutralized with 400 mM Tris–HCl, pH 7.4 and blocked in 5% BSA and 10% goat serum at RT for 1 h. The fibers were first immunostained with rat anti-CIdU antibody (1:100, ab6326, Abcam) for 1 h, washed in PBST (PBS+Tween 20), and incubated with AlexaFluor 647-conjugated anti-rat IgG (1:100, A-21247, Molecular Probes) for another 1 h followed by stringent PBST wash. Similarly, the slides were stained with mouse anti-IdU antibody (1:40, # 347580, BD Pharmingen) followed by incubation with AlexaFluor 488-conjugated anti-mouse IgG (1:100, A-11001, Molecular Probes). Slides were mounted with ProLong Gold antifade mountant (P36930, Invitrogen). Labeled DNA fibers were examined using Leica TCS SP8 system (LAS X software) with a 63× (oil) Plan Apochromat objective lens (NA 1.4). HeNe laser (633 nm) and argon laser (488 nm) were used for the detection of CldU- and IdU-labeled patches respectively. For origin firing calculation, we calculated the percentage of 1st label origin structures (green-red-green) among the total number of red label fibers using ImageJ software (http://rsb.info.nih.gov/ij/). Approximately 200–300 red label fibers from each sample were scored and analyzed for origin firing events in three independent experiments. For fork speed determination, length of the unidirectional ongoing fork (red-green) was measured in μm using Leica LAS AF Lite software and converted into kb using the formula 1 μm = 2.59 kb [48]. For fork speed analysis, ~70 to 100 untangled fibers were scored from each sample in three independent experiments.

Flow cytometry

For cell cycle analysis, cells were first treated with 0.5 μg/ml of doxycycline for 48 h and subsequently ~1 × 10^6 cells were synchronized at G1/S-phase by double-thymidine (2.5 mM) block. Cells released in fresh medium were harvested at different time points and fixed in chilled ethanol (70% v/v) overnight at 4°C. Fixed cells were stained in 1× PBS containing 100 μg/ml propidium iodide (P-4170, Sigma) and 20 μg/ml RNase A (# 12091-039, Invitrogen) following FACS analysis in BD LSRFortessa using BD FACSDiva 6.2 software. BrdU pulse chase assay was performed using FITC BrdU flow kit (#559619, BD Pharmingen) according to the manufacturer's protocol.

Clonogenicity assay

H1299 cells harboring tet-regulated control or *CDC7* shRNA was transfected with 4 μg of either pCMV-vector or with plasmids encoding wild-type and mutant p53. Transfected cells were selected by G418 for 15–30 days, and stable colonies were pooled to generate control vector, wild-type and mutant p53-expressing stable cells bearing control or *CDC7* shRNA. Cells were seeded (~1,500 cells) on 6-cm dishes and allowed to grow in complete medium containing doxycycline (0.25 μg/ml, D9891, Sigma) until the colonies become visible (~2 weeks). The colonies were stained in 0.1% methylene blue, photographed, and counted using ImageJ software (http://rsb.info.nih.gov/ij/).

Soft agar assay

Soft agar assay was performed as described previously [49]. Cells were allowed to form colonies for 2–3 weeks in presence of doxycycline (0.25 μg/ml). Colony images were taken using Olympus IX71 microscope at 20× magnification, and visible colonies were counted using ImageJ software (http://rsb.info.nih.gov/ij/).

Drug sensitivity assay

Cells transfected with either control or *CDC7* siRNA were treated with drugs 24 h post-transfection. After 48 h of drug treatment, the assay was performed using WST-1 cell proliferation reagent (Roche, #05015944001) according to the manufacturer's protocol.

In vivo tumorigenicity experiments

The animal studies were performed in compliance with the guidelines of the Institutional Animal Ethics Committee of National Centre for Cell Science, India. Briefly, 2×10^6 control (EV) and mutant p53-R175H-expressing H1299 cells harboring doxycycline-inducible either control shRNA or *CDC7* shRNA were injected subcutaneously into the dorsal side of the flanks of 6-week-old male NOD/SCID mice. Ten mice were divided randomly into two groups with one group injected with EV/shCtrl and EV/sh*CDC7* cells and the other group injected with mutant p53-R175H/shCtrl and mutant p53-R175H/sh*CDC7* cells into left and right flank, respectively. Mice were kept on doxycycline-containing water (2 mg/ml) supplemented with 5% sucrose when palpable tumors appeared. After specific time period, mice were sacrificed; tumors were excised and weighed. Tumor volumes were estimated using the formula: $\pi/6[(d1*d2)^{3/2}]$, where d1 and d2 represent two different diameters of the tumor mass. To investigate the effect of *CDC7* knockdown on increased chemoresistance phenotype of mutant p53-bearing cancer cells *in vivo*, 5×10^6 SW480 cells harboring doxycycline-inducible control or *CDC7* shRNA were injected into dorsal side of left and right flank of 6-week-old male NOD/SCID mice, respectively. Two such groups each containing four animals were kept on doxycycline supplementation once palpable tumors appeared. Further, the first group was injected with vehicle control DPBS (Invitrogen) intraperitoneally (i.p.), whereas the second group was injected with 5-FU i.p.

Immunohistochemical analyses of xenograft tumor tissues

Tissue sections were deparaffinized, hydrated, subjected to antigen retrieval using citrate buffer (pH = 6.0), and probed with specific antibodies (1:50) overnight at 4°C in a humid chamber. The sections were washed and incubated with HRP-conjugated anti-mouse secondary antibody (1:500). 3, 3′ diaminobenzidine (DAB) was used as chromogen. The sections were subsequently counterstained with hematoxylin, and photographs were taken using Leica DM1000 system (LAS EZ version 1.5.0) at 40× magnification.

Bioinformatics and statistical analyses

Level 3 RNA sequencing data of 230 resected lung adenocarcinomas was obtained from TCGA data portal (https://tcga-data.nci.nih.gov/docs/publications/luad_2014/). The p53 mutation data of the respective patients were obtained from the published article describing the study [50]. Clinical data of the patients were obtained from cBioPortal (http://cbioportal.org) [51,52]. On the basis of p53 mutation, patients were classified into two groups, patients with wild-type p53 and those with missense mutant p53 with reported *gain-of-function* (GOF) properties [35,53] (Dataset EV1). Differential gene expression analysis between wild-type and GOF mutant p53 patients was carried out using Bioconductor package LIMMA. Pathway enrichment analysis was done using ingenuity pathways analysis (IPA; https://analysis.ingenuity.com) tool. For survival analysis, out of 230 lung adenocarcinoma patients, we considered 195 patients whose overall survival time was available in TCGA clinical data set (Dataset EV3). We eliminated remaining 35 patients whose overall survival time was either not available (NA) or given as time zero (0; Dataset EV4). Kaplan–Meier analyses were done using GraphPad Prism version 5.03. Multivariate survival analysis was done by Cox proportional hazard model in SPSS version 16.0. Student's two-tailed *t*-test with confidence interval of 95% was applied for analyzing experiments unless otherwise specified, and *P*-values < 0.05 were considered significant.

Expanded View for this article is available online.

Acknowledgements

We thank Prof. Varda Rotter (Weizmann Institute of Science, Rehovot, Israel) and Prof. Tanya Das (Bose Institute, Kolkata, India) for kindly providing us with the H1299/EV, H1299/R175H, and basic H1299 cell lines, respectively. We thank Prof. Giovanni Blandino (Regina Elena National Cancer Institute, Italy) and Prof. Luis Alfonso Martinez (Stony Brook University, NY, USA) for kindly providing us with mutant p53-R175H domain mutants. We thank Prof. Bert Vogelstein (Johns Hopkins University, MD, USA) and Prof. Corrado Santocanale (National University of Ireland, Galway, Ireland) for kindly providing us with mutant p53 expression plasmids and GST-Mcm2 plasmid clone, respectively. We thank Dr. Soma Banerjee (IPGMER, Kolkata, India) for providing us with reagents. We thank Dr. Uday Bandyopadhyay (CSIR-Indian Institute of Chemical Biology, India) for providing us with Leica TCS SP8 system. We thank Mr. Tanmoy Dalui and Sounak Bhattacharya (CSIR-Indian Institute of Chemical Biology, India) for their assistance in flow cytometry and confocal microscopy, respectively. This work was supported by CSIR-Mayo Clinic Collaboration for Innovation and Translational Research Grant CMPP-08 and CSIR-NMITLI project Grant TLP 0007 awarded to S. Roychoudhury.

Author contributions

AD and SR conceived and designed the study. AD, DG, and AP performed the experiments. AD, DG, and TB analyzed DNA fiber experiment data. SD, RB, MG, and AD performed xenograft experiments, and GCK analyzed xenograft data. SG, AR, SKA, PD, RC, MD, and CKP analyzed the data. AD and SR wrote the manuscript.

Conflict of interest

The authors declare that they have no conflict of interest.

References

1. Olivier M, Hollstein M, Hainaut P (2010) TP53 mutations in human cancers: origins, consequences, and clinical use. *Cold Spring Harb Perspect Biol* 2: a001008
2. Freed-Pastor WA, Prives C (2012) Mutant p53: one name, many proteins. *Genes Dev* 26: 1268 – 1286
3. Mello SS, Attardi LD (2013) Not all p53 gain-of-function mutants are created equal. *Cell Death Differ* 20: 855 – 857
4. Li Y, Prives C (2007) Are interactions with p63 and p73 involved in mutant p53 gain of oncogenic function? *Oncogene* 26: 2220 – 2225
5. Blandino G, Levine AJ, Oren M (1999) Mutant p53 gain of function: differential effects of different p53 mutants on resistance of cultured cells to chemotherapy. *Oncogene* 18: 477 – 485
6. Walerych D, Lisek K, Sommaggio R, Piazza S, Ciani Y, Dalla E, Rajkowska K, Gaweda-Walerych K, Ingallina E, Tonelli C *et al* (2016) Proteasome machinery is instrumental in a common gain-of-function program of the p53 missense mutants in cancer. *Nat Cell Biol* 18: 897 – 909
7. Polotskaia A, Xiao G, Reynoso K, Martin C, Qiu WG, Hendrickson RC, Bargonetti J (2015) Proteome-wide analysis of mutant p53 targets in breast cancer identifies new levels of gain-of-function that influence PARP, PCNA, and MCM4. *Proc Natl Acad Sci USA* 112: E1220 – E1229
8. Abbas T, Keaton MA, Dutta A (2013) Genomic instability in cancer. *Cold Spring Harb Perspect Biol* 5: a012914
9. Suzuki M, Takahashi T (2013) Aberrant DNA replication in cancer. *Mutat Res* 743–744: 111 – 117
10. Valenzuela MS, Hu L, Lueders J, Walker R, Meltzer PS (2012) Broader utilization of origins of DNA replication in cancer cell lines along a 78 kb region of human chromosome 2q34. *J Cell Biochem* 113: 132 – 140
11. Bonte D, Lindvall C, Liu H, Dykema K, Furge K, Weinreich M (2008) Cdc7-Dbf4 kinase overexpression in multiple cancers and tumor cell lines is correlated with p53 inactivation. *Neoplasia* 10: 920 – 931
12. Masai H, Arai K (2002) Cdc7 kinase complex: a key regulator in the initiation of DNA replication. *J Cell Physiol* 190: 287 – 296
13. Labib K (2010) How do Cdc7 and cyclin-dependent kinases trigger the initiation of chromosome replication in eukaryotic cells? *Genes Dev* 24: 1208 – 1219
14. Yamada M, Masai H, Bartek J (2014) Regulation and roles of Cdc7 kinase under replication stress. *Cell Cycle* 13: 1859 – 1866
15. Montagnoli A, Moll J, Colotta F (2010) Targeting cell division cycle 7 kinase: a new approach for cancer therapy. *Clin Cancer Res* 16: 4503 – 4508
16. Streubel G, Bouchard C, Berberich H, Zeller MS, Teichmann S, Adamkiewicz J, Muller R, Klempnauer KH, Bauer UM (2013) PRMT4 is a novel coactivator of c-Myb-dependent transcription in haematopoietic cell lines. *PLoS Genet* 9: e1003343
17. Shi L, Ko S, Kim S, Echchgadda I, Oh TS, Song CS, Chatterjee B (2008) Loss of androgen receptor in aging and oxidative stress through Myb protooncoprotein-regulated reciprocal chromatin dynamics of p53 and poly(ADP-ribose) polymerase PARP-1. *J Biol Chem* 283: 36474 – 36485
18. Tanikawa J, Nomura T, Macmillan EM, Shinagawa T, Jin W, Kokura K, Baba D, Shirakawa M, Gonda TJ, Ishii S (2004) p53 suppresses c-Myb-induced trans-activation and transformation by recruiting the corepressor mSin3A. *J Biol Chem* 279: 55393 – 55400
19. Di Agostino S, Sorrentino G, Ingallina E, Valenti F, Ferraiuolo M, Bicciato S, Piazza S, Strano S, Del Sal G, Blandino G (2016) YAP enhances the pro-proliferative transcriptional activity of mutant p53 proteins. *EMBO Rep* 17: 188 – 201
20. Do PM, Varanasi L, Fan S, Li C, Kubacka I, Newman V, Chauhan K, Daniels SR, Boccetta M, Garrett MR *et al* (2012) Mutant p53 cooperates with ETS2 to promote etoposide resistance. *Genes Dev* 26: 830 – 845
21. Tsuji T, Ficarro SB, Jiang W (2006) Essential role of phosphorylation of MCM2 by Cdc7/Dbf4 in the initiation of DNA replication in mammalian cells. *Mol Biol Cell* 17: 4459 – 4472
22. Montagnoli A, Valsasina B, Brotherton D, Troiani S, Rainoldi S, Tenca P, Molinari A, Santocanale C (2006) Identification of Mcm2 phosphorylation sites by S-phase-regulating kinases. *J Biol Chem* 281: 10281 – 10290
23. Zou L, Stillman B (2000) Assembly of a complex containing Cdc45p, replication protein A, and Mcm2p at replication origins controlled by S-phase cyclin-dependent kinases and Cdc7p-Dbf4p kinase. *Mol Cell Biol* 20: 3086 – 3096
24. Zhong Y, Nellimoottil T, Peace JM, Knott SR, Villwock SK, Yee JM, Jancuska JM, Rege S, Tecklenburg M, Sclafani RA *et al* (2013) The level of origin firing inversely affects the rate of replication fork progression. *J Cell Biol* 201: 373 – 383
25. Petermann E, Woodcock M, Helleday T (2010) Chk1 promotes replication fork progression by controlling replication initiation. *Proc Natl Acad Sci USA* 107: 16090 – 16095
26. Di Paola D, Rampakakis E, Chan MK, Arvanitis DN, Zannis-Hadjopoulos M (2010) Increased origin activity in transformed versus normal cells: identification of novel protein players involved in DNA replication and cellular transformation. *Nucleic Acids Res* 38: 2314 – 2331
27. Alam SK, Yadav VK, Bajaj S, Datta A, Dutta SK, Bhattacharyya M, Bhattacharya S, Debnath S, Roy S, Boardman LA *et al* (2016) DNA damage-induced ephrin-B2 reverse signaling promotes chemoresistance and drives EMT in colorectal carcinoma harboring mutant p53. *Cell Death Differ* 23: 707 – 722
28. Wattel E, Preudhomme C, Hecquet B, Vanrumbeke M, Quesnel B, Dervite I, Morel P, Fenaux P (1994) p53 mutations are associated with resistance to chemotherapy and short survival in hematologic malignancies. *Blood* 84: 3148 – 3157
29. Datta A, Dey S, Das P, Alam SK, Roychoudhury S (2016) Transcriptome profiling identifies genes and pathways deregulated upon floxuridine treatment in colorectal cancer cells harboring GOF mutant p53. *Genom Data* 8: 47 – 51
30. Muller PA, Vousden KH (2013) p53 mutations in cancer. *Nat Cell Biol* 15: 2 – 8
31. Frum RA, Deb S, Deb SP (2013) Use of the DNA fiber spreading technique to detect the effects of mutant p53 on DNA replication. *Methods Mol Biol* 962: 147 – 155
32. Guo B, Romero J, Kim BJ, Lee H (2005) High levels of Cdc7 and Dbf4 proteins can arrest cell-cycle progression. *Eur J Cell Biol* 84: 927 – 938
33. Fischer M, Quaas M, Wintsche A, Muller GA, Engeland K (2014) Polo-like kinase 4 transcription is activated via CRE and NRF1 elements, repressed

by DREAM through CDE/CHR sites and deregulated by HPV E7 protein. *Nucleic Acids Res* 42: 163 – 180

34. Spurgers KB, Gold DL, Coombes KR, Bohnenstiehl NL, Mullins B, Meyn RE, Logothetis CJ, McDonnell TJ (2006) Identification of cell cycle regulatory genes as principal targets of p53-mediated transcriptional repression. *J Biol Chem* 281: 25134 – 25142
35. Muller PA, Vousden KH (2014) Mutant p53 in cancer: new functions and therapeutic opportunities. *Cancer Cell* 25: 304 – 317
36. Strano S, Dell'Orso S, Di Agostino S, Fontemaggi G, Sacchi A, Blandino G (2007) Mutant p53: an oncogenic transcription factor. *Oncogene* 26: 2212 – 2219
37. Ramsay RG, Gonda TJ (2008) MYB function in normal and cancer cells. *Nat Rev Cancer* 8: 523 – 534
38. Yamada M, Watanabe K, Mistrik M, Vesela E, Protivankova I, Mailand N, Lee M, Masai H, Lukas J, Bartek J (2013) ATR-Chk1-APC/CCdh1-dependent stabilization of Cdc7-ASK (Dbf4) kinase is required for DNA lesion bypass under replication stress. *Genes Dev* 27: 2459 – 2472
39. Hills SA, Diffley JF (2014) DNA replication and oncogene-induced replicative stress. *Curr Biol* 24: R435 – R444
40. Wong PG, Winter SL, Zaika E, Cao TV, Oguz U, Koomen JM, Hamlin JL, Alexandrow MG (2011) Cdc45 limits replicon usage from a low density of preRCs in mammalian cells. *PLoS One* 6: e17533
41. Wu PY, Nurse P (2009) Establishing the program of origin firing during S phase in fission Yeast. *Cell* 136: 852 – 864
42. Duronio RJ (2012) Developing S-phase control. *Genes Dev* 26: 746 – 750
43. Montagnoli A, Valsasina B, Croci V, Menichincheri M, Rainoldi S, Marchesi V, Tibolla M, Tenca P, Brotherton D, Albanese C *et al* (2008) A Cdc7 kinase inhibitor restricts initiation of DNA replication and has antitumor activity. *Nat Chem Biol* 4: 357 – 365
44. Swords R, Mahalingam D, O'Dwyer M, Santocanale C, Kelly K, Carew J, Giles F (2010) Cdc7 kinase - a new target for drug development. *Eur J Cancer* 46: 33 – 40
45. Weisz L, Zalcenstein A, Stambolsky P, Cohen Y, Goldfinger N, Oren M, Rotter V (2004) Transactivation of the EGR1 gene contributes to mutant p53 gain of function. *Can Res* 64: 8318 – 8327
46. Montagnoli A, Bosotti R, Villa F, Rialland M, Brotherton D, Mercurio C, Berthelsen J, Santocanale C (2002) Drf1, a novel regulatory subunit for human Cdc7 kinase. *EMBO J* 21: 3171 – 3181
47. Banerjee T, Sommers JA, Huang J, Seidman MM, Brosh RM Jr (2015) Catalytic strand separation by RECQ1 is required for RPA-mediated response to replication stress. *Curr Biol* 25: 2830 – 2838
48. Henry-Mowatt J, Jackson D, Masson JY, Johnson PA, Clements PM, Benson FE, Thompson LH, Takeda S, West SC, Caldecott KW (2003) XRCC3 and Rad51 modulate replication fork progression on damaged vertebrate chromosomes. *Mol Cell* 11: 1109 – 1117
49. Bajaj S, Alam SK, Roy KS, Datta A, Nath S, Roychoudhury S (2016) E2 Ubiquitin-conjugating enzyme, UBE2C gene, is reciprocally regulated by wild-type and gain-of-function mutant p53. *J Biol Chem* 291: 14231 – 14247
50. Cancer Genome Atlas Research Network (2014) Comprehensive molecular profiling of lung adenocarcinoma. *Nature* 511: 543 – 550
51. Cerami E, Gao J, Dogrusoz U, Gross BE, Sumer SO, Aksoy BA, Jacobsen A, Byrne CJ, Heuer ML, Larsson E *et al* (2012) The cBio cancer genomics portal: an open platform for exploring multidimensional cancer genomics data. *Cancer Discov* 2: 401 – 404
52. Gao J, Aksoy BA, Dogrusoz U, Dresdner G, Gross B, Sumer SO, Sun Y, Jacobsen A, Sinha R, Larsson E *et al* (2013) Integrative analysis of complex cancer genomics and clinical profiles using the cBioPortal. *Sci Signal* 6: pl1
53. Petitjean A, Mathe E, Kato S, Ishioka C, Tavtigian SV, Hainaut P, Olivier M (2007) Impact of mutant p53 functional properties on TP53 mutation patterns and tumor phenotype: lessons from recent developments in the IARC TP53 database. *Hum Mutat* 28: 622 – 629

